

Perspective

Self-Healing Dyes – Keeping The Promise?

Michael Isselstein, Lei Zhang, Viktorija Glembockyte, Oliver Brix, Gonzalo Cosa, Philip Tinnefeld, and Thorben Cordes

J. Phys. Chem. Lett., Just Accepted Manuscript • DOI: 10.1021/acs.jpclett.9b03833 • Publication Date (Web): 13 May 2020

Downloaded from pubs.acs.org on May 27, 2020

Just Accepted

“Just Accepted” manuscripts have been peer-reviewed and accepted for publication. They are posted online prior to technical editing, formatting for publication and author proofing. The American Chemical Society provides “Just Accepted” as a service to the research community to expedite the dissemination of scientific material as soon as possible after acceptance. “Just Accepted” manuscripts appear in full in PDF format accompanied by an HTML abstract. “Just Accepted” manuscripts have been fully peer reviewed, but should not be considered the official version of record. They are citable by the Digital Object Identifier (DOI®). “Just Accepted” is an optional service offered to authors. Therefore, the “Just Accepted” Web site may not include all articles that will be published in the journal. After a manuscript is technically edited and formatted, it will be removed from the “Just Accepted” Web site and published as an ASAP article. Note that technical editing may introduce minor changes to the manuscript text and/or graphics which could affect content, and all legal disclaimers and ethical guidelines that apply to the journal pertain. ACS cannot be held responsible for errors or consequences arising from the use of information contained in these “Just Accepted” manuscripts.

Self-Healing Dyes – Keeping the Promise?

Michael Isselstein^{1,#}, Lei Zhang^{1,#}, Viktorija Glembockyte^{2,3,#}, Oliver Brix¹, Gonzalo Cosa³, Philip Tinnefeld², and Thorben Cordes^{1,*}

¹ Physical and Synthetic Biology, Faculty of Biology, Ludwig-Maximilians-Universität München, Großhadernerstr. 2-4, 82152 Planegg-Martinsried, Germany

² Department of Chemistry and Center for NanoScience, Ludwig-Maximilians-Universität München, Butenandtstr. 5-13, Haus E 81377 München, Germany

³ Department of Chemistry and Quebec Centre for Applied Materials (QCAM), McGill University, 801 Sherbrooke Street W., H3A 0B8 Montreal, Quebec, Canada

equal contribution; *corresponding author email: cordes@bio.lmu.de

Abstract: Self-healing dyes have emerged as a new promising class of fluorescent labels. They consist of two units, a fluorescent dye and a photostabilizer. The latter heals whenever the fluorescent dye is endangered of taking a reaction pathway towards photobleaching. We describe the underlying concepts, summarize the developmental history and state-of-the-art, including latest applications in high-resolution microscopy, live-cell and single-molecule imaging. We further discuss remaining limitations, which are (i) lower photostabilization of most self-healing dyes when compared to solution additives, (ii) limited mechanistic understanding on the influence of the biochemical environment and molecular oxygen on self-healing, and (iii) the lack of cheap and facile bioconjugation strategies. Finally, we provide ideas on how to further advance self-healing dyes, show new data on redox blinking caused by double-stranded DNA and highlight forthcoming work on intramolecular photostabilization of fluorescent proteins.

1
2
3
4
5
6
7
8
9
10
11
12
13
14
15
16
17
18
19
20
21
22
23
24
25
26
27
28
29
30
31
32
33
34
35
36
37
38
39
40
41
42
43
44
45
46
47
48
49
50
51
52
53
54
55
56
57
58
59
60

Fluorescence microscopy, including single-molecule and super-resolution imaging, has evolved as a powerful tool to study the structure and dynamics of biological systems *in vitro* and *in vivo* down to the molecular level. Here an optimal performance of the contrast agents—fluorescent dyes and proteins—is achieved via suppression of undesired long-lived and reactive fluorophore states generated upon the continuous excitation typical of single-molecule studies.¹⁻² This suppression can be realized via oxygen removal³⁻⁵ in combination with the addition of photostabilizing compounds P *in vitro* that quench, e.g., triplet- or radical states (Figure 1a; triplet T₁).⁶⁻⁷ Here, a fluorophore F is protected against damage in an intermolecular approach (Figure 1a), where the triplet-state is depleted via diffusional collisions resulting in photophysical or photochemical quenching. Photophysical triplet-state-quenchers, such as cyclooctatetraene (COT)⁸⁻¹⁰, diphenylhexatriene¹¹, or Ni²⁺ ions¹²⁻¹³, rely on energy transfer between the fluorescent dye (donor) and the quencher (acceptor).

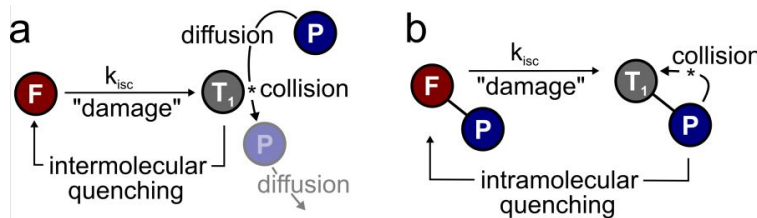


Figure 1. Schematic illustration of interactions between photostabilizers and fluorophores (where T₁ is the triplet state of a fluorophore) via (a) intermolecular and (b) intramolecular quenching processes.

Reprinted from ref. ¹⁴ with permission.

Photochemical triplet-state quenching requires a combination of redox-active agents (e.g., Trolox (TX),^{2,15} ascorbic acid (AA^{3,7,16}), ferrocene,¹⁷ nitrobenzylalcohol (NBA),¹⁰ nitrophenylalanine (NPA),¹⁸⁻¹⁹ nitrophenylacetic acid (NPAA),¹⁸ methylviologen (MV),^{7,16} Trolox-quinone¹⁵). Triplet states are then quenched via photoinduced electron transfer (PET) resulting in the formation of a radical anion or cation. Simultaneous use of both reducing and oxidizing agents (referred to as ROXS system⁷) allows to quench all newly formed radical intermediates and to restore the ground state of the dye via consecutive redox reactions.⁷

High concentrations of (toxic) photostabilizers are however required for both

1
2
3 55 photophysical and photochemical quenching, to ensure an effective depletion of
4 56 reactive states. Such conditions are often incompatible with certain biological settings
5 57 such as live cell imaging, since organic (hydrophobic) compounds can perturb
6 58 biological structures and/or function.²⁰ As illustrated in Figure 1a, intermolecular
7 59 photostabilizers require direct collisions with the fluorophore, restricting their use to
8 60 systems where the dyes are solvent accessible.^{14,21}

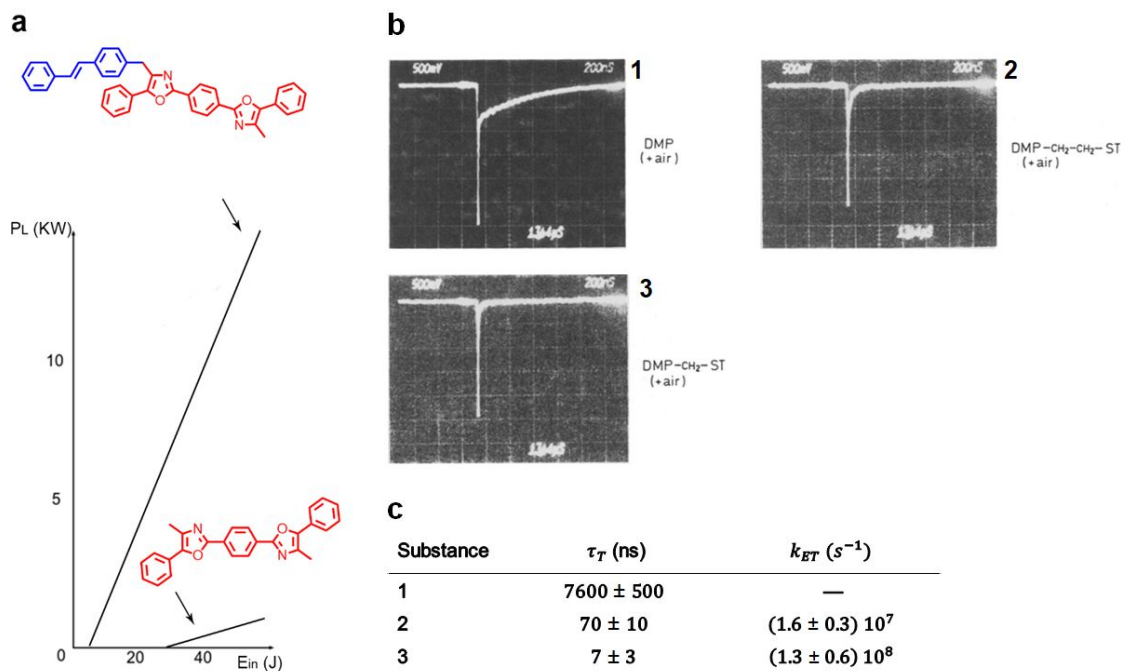
9
10 61 An alternative approach, which is the focus of this Perspective, uses direct
11 62 conjugation of photostabilizing compounds to the fluorophore, thereby creating high
12 63 local concentrations of photostabilizer around the fluorophore. As illustrated in Figure
13 64 1b, this allows intramolecular quenching of triplet or radical states. Such a strategy
14 65 obviates the need for complex buffer systems, rendering these dyes with
15 66 intramolecular photostabilization “self-healing”²⁸ and thus compatible with diverse
16 67 biological systems,^{19,22-25} even when the fluorescent dyes are inaccessible to
17 68 solution-based stabilizers.

18
19 69 In this Perspective, we describe the concepts, history²⁶⁻²⁷ and state of the art of
20 70 self-healing dyes^{19,22-25,28-30} with a focus on the current mechanistic understanding
21 71 and applications. For this, we summarize how, over the past years, the photophysical
22 72 properties of self-healing dyes have been optimized,^{14,18,31-32} versatile bioconjugation
23 73 strategies for different fluorophore types, photostabilizers and biomolecules were
24 74 established,^{19,33} important mechanistic insights were obtained³⁴ and exciting
25 75 applications, e.g., in super-resolution imaging^{19,35} were presented. Most importantly,
26 76 however, we go beyond the current state of the art and discuss remaining limitations
27 77 and challenges that have to be overcome to further improve this new class of dyes.
28
29 78 In our view, remaining key limitations are (i) lower photostabilization efficiency of
30 79 most self-healing dyes when compared to the pristine dye in combination with
31 80 solution additives, (ii) limited mechanistic understanding on the influence of the
32 81 biochemical environment and (iii) molecular oxygen on self-healing, and (iv) the lack
33 82 of cheap and facile bioconjugation strategies. Finally, we provide new data and
34 83 information on self-healing processes in double-stranded DNA with differing base
35 84 sequences and preliminary data toward use of intramolecular photoprotection of

1
2
3 85 fluorescent proteins.
4
5
6

7 87 **2. History, development and state of the art of self-healing dyes**
8
9

10 88 The concept of enhancing the photostability of fluorescent dyes via linking triplet
11 89 state-quenchers was proposed, experimentally realized and verified in the early
12 90 1980s.^{26-27,98} Lüttke and co-workers linked 1,4-bis(5-phenyloxazol-2-yl)benzene
13 91 (POPOP) and its derivatives to stilbene with the goal to quench triplet states (Figure
14 92 2a). These self-healing POPOP-stilbene constructs showed very good performance
15 93 as lasing medium in dye lasers (Figure 2a) and were the first self-healing dyes with
16 94 intramolecular photostabilization.²⁷

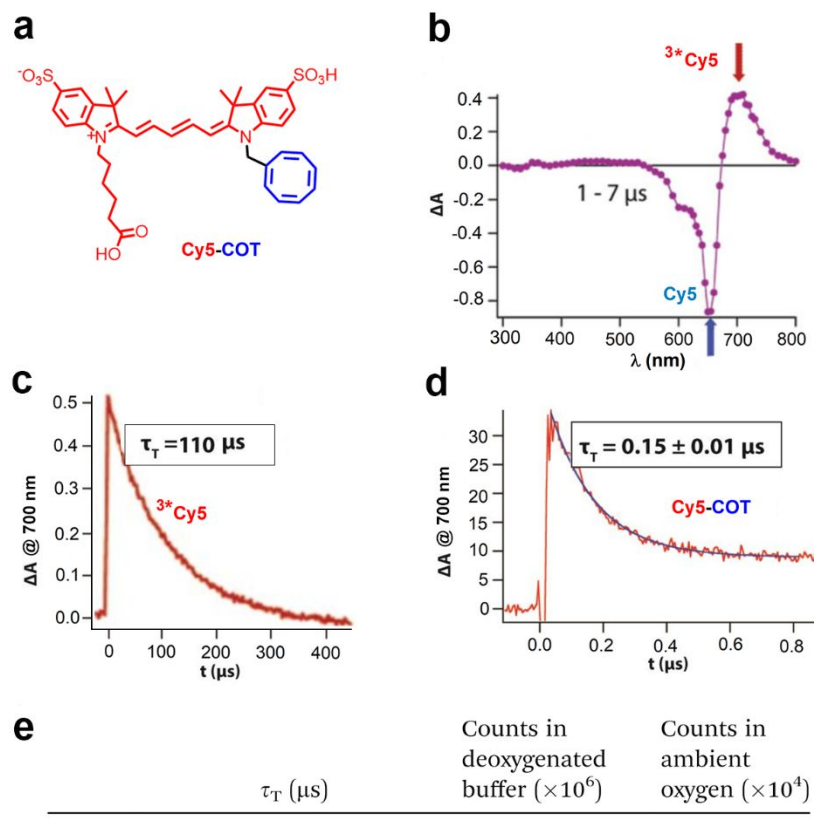


96 **Figure 2.** (a) Dye-laser output power (P_L) versus electrical input energy (E_{in}) using dimethyl-POPOP
97 (DMP) and DMP-stilbene as laser-dye; data from ref. ²⁷. (b) Oscillograms of transient absorption of DMP
98 (1) and DMP-stilbene compounds (2,3). All compounds were measured in dioxane solution and were
99 air-equilibrated. Dye 2 has two CH₂ groups, whereas dye 3 has one CH₂ group between DMP and *trans*-
100 stilbene; oscillograms taken from ref. ³⁶. (c) Measured triplet lifetimes τ_T and calculated TT-energy
101 transfer rates k_{ET} . A decreasing distance between laser dye and triplet-quenching molecule results in
102 increasing k_{ET} rates; data from ref. ³⁶.

103
104 Schäfer et al. experimentally confirmed the proposed triplet-state quenching
105 through triplet-triplet energy transfer in dimethyl-POPOP (DMP) covalently linked to
106 *trans*-stilbene in 1982 via transient absorption spectroscopy (Figure 2b).³⁶ It was also

1
2
3
4 107 possible to calculate the intramolecular triplet-triplet energy transfer rates k_{ET} by
5 108 measuring the triplet lifetimes of the DMP-triplet-quencher compounds. Furthermore,
6 109 Schäfer et al. demonstrated decreasing triplet-triplet energy transfer times with
7 110 decreasing distances between laser dye and triplet-quencher (Figure 2c). With that,
8 111 both groups established the mechanistic basis for self-healing dyes.
9
10
11
12

13 112 The idea to utilize intramolecular triplet state quenching for photostabilization
14 113 was revived by Blanchard in 2012²², by Cordes in 2013²⁴ and by other groups in
15 114 subsequent years.^{30,37} These papers demonstrated improved photophysical
16 115 properties of self-healing dyes and the possibility to use intramolecular
17 116 photostabilizers for a variety of dyes from distinct structural classes.^{14,19,33} A direct
18 117 correlation between triplet state quenching and reduced photobleaching was
19 118 observed directly in Cy5 conjugates (Figure 3a) using transient absorption
20 119 spectroscopy, TAS (Figure 2b, 3b-d).^{23,31} In self-healing dyes, a much shorter triplet-
21 120 state-lifetime was observed for example for Cy5-COT conjugation (Figure 3d/e) in
22 121 combination with increased photostability (Figure 3e).



122

1
2
3 123 **Figure 3.** (a) Structure of self-healing Cy5-COT; (b) Transient absorption spectra of Cy5 in
4 124 deoxygenated acetonitrile solution; triplet sensitization via covalent linkage of 9-oxothioxanthene (OTX);
5 125 (c) Transient absorption kinetics of Cy5 at 700 nm (corresponding to absorbance of ${}^3\text{Cy}5$) after pulsed
6 126 laser excitation of Cy5 in deoxygenated acetonitrile solution; (d) Transient absorption kinetics at 700 nm
7 127 after pulsed laser excitation of self-healing Cy5-COT in deoxygenated acetonitrile solution; (e) Triplet-
8 128 state-lifetime (τ_T) and average number of photons detected prior to fluorophore photobleaching in
9 129 deoxygenated buffers as well as ambient oxygen condition recorded for Cy5 and Cy5-COT on double
10 130 stranded DNA. Panels b-f were reprinted from ref.³¹ with permission.
11
12
13
14
15

16 132 Over the past years, TAS,^{23,31} single-molecule total internal reflection microscopy
17 133 (smTIRF),^{14,18-19,22,24,28,30-33,35,38} as well as confocal microscopy^{14,19,24,32,35} were
18 134 important spectroscopic tools used for characterization of the photophysical
19 135 properties of self-healing dyes in comparison to their non-stabilized counterparts in
20 136 various buffer systems. TAS can directly trace key photochemical and photophysical
21 137 intermediates and their spectra with high time-resolution (Figure 3b-d); in these
22 138 experiments fluorescent dyes are analyzed freely-diffusing in bulk solution at high
23 139 concentrations.³⁹⁻⁴⁰ smTIRF and confocal microscopy, on the other hand, enable
24 140 collection of time-resolved fluorescence trajectories of individual fluorescent
25 141 molecules (Figure 4a), allowing the extraction of photophysical properties of the
26 142 dyes, such as their photobleaching lifetime, fluorescence intensity (brightness), total
27 143 photon output before photobleaching, signal-to-noise ratio, as well as their
28 144 fluorescence lifetimes in different intensity regimes at the single-molecule
29 145 level.^{14,22,28,30,32,35} For this, fluorophores are typically immobilized on a streptavidin-
30 146 functionalized coverslip via bioconjugation with biotin-modified double-stranded DNA-
31 147 scaffolds (Figure 4a), via proteins^{30,41-42} or others and imaged in the presence of an
32 148 enzymatic oxygen scavenging buffer to remove molecular oxygen.^{7,15,43-44}
33
34
35
36
37
38
39
40
41
42
43
44
45
46
47
48
49
50
51
52
53
54
55
56
57
58
59
60

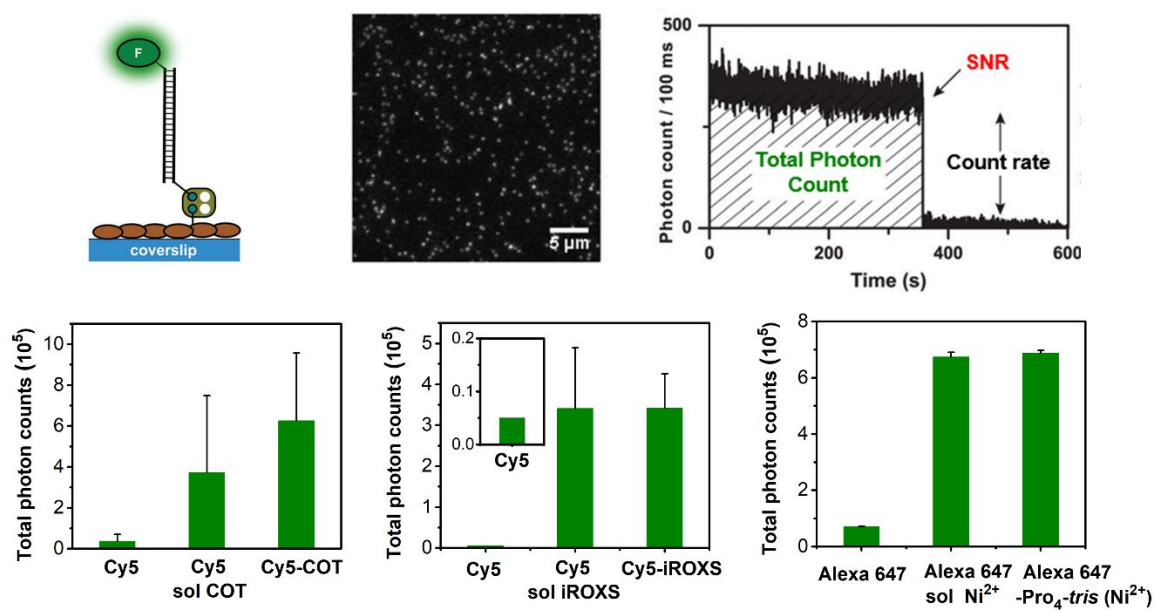


Figure 4: (a) Scheme of fluorophores immobilized on a streptavidin-functionalized coverslip via bioconjugation with biotin-modified double-stranded DNA-scaffolds. (b) Coverage of a typical sample area obtained with TIRF microscopy showing individual fluorophores. (c) Fluorescence time trace of an individual fluorophore allowing to extract count rate, SNR ratio and the total number of detected photons. (d-f) Total photon counts detected from individual fluorophores in deoxygenated buffer before photobleaching of (d) Cy5, Cy5 in buffer containing 1 mM COT (sol COT), and Cy5 conjugated to a single COT; data from ref.²²; (e) Cy5, Cy5 in buffer containing 1 mM iROXS (a conjugation of NPA and TX), and Cy5 in proximity to a single iROXS molecule, data from ref.³²; (f) Alexa 647, Alexa 647 with 0.1 mM Ni²⁺ as solution additive, and Alexa 647 with three proximal Ni²⁺ ions in a *tris*NTA moiety, data from ref.³⁰.

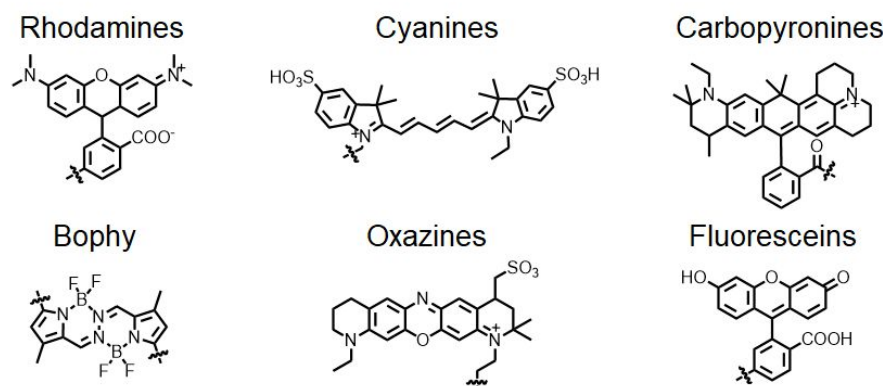
Established building blocks for self-healing dyes

Over the past years, a variety of fluorophore-stabilizer conjugates have been synthesized and tested using different photostabilization agents and classes of fluorescent dyes (Figure 5).^{14,18-19,22-24,31-33,45} These conjugates include rhodamines (ATTO565, Alexa555, Alexa633, Alexa568, KK114, STAR635P, TMR);^{14,19,33,35} cyanines (Cy2, Cy3, Cy3.5, Cy5, Cy5.5, Dy549, Cy7);^{14,18-19,22-24,28,31-33} carbopyronines (ATTO647N),^{14,19,33,35} bophy-dyes,⁴⁵ oxazines (ATTO655),³³ and fluoresceins³³ with representative examples shown in Figure 4a. Among all the conjugates, the photostability of the fluorophore was enhanced when coupled to the photostabilizer with the exception of oxazines and fluoresceins.³³ The self-healing dye constructs included photostabilizers such as COT,^{14,22-23,31,33} TX,^{19,22-24,32} nitrophenyl-based stabilizers,^{14,18-19,22-23,32,35} BHT,⁴⁵ Ni²⁺ ions,³⁰ as well as a combined molecule

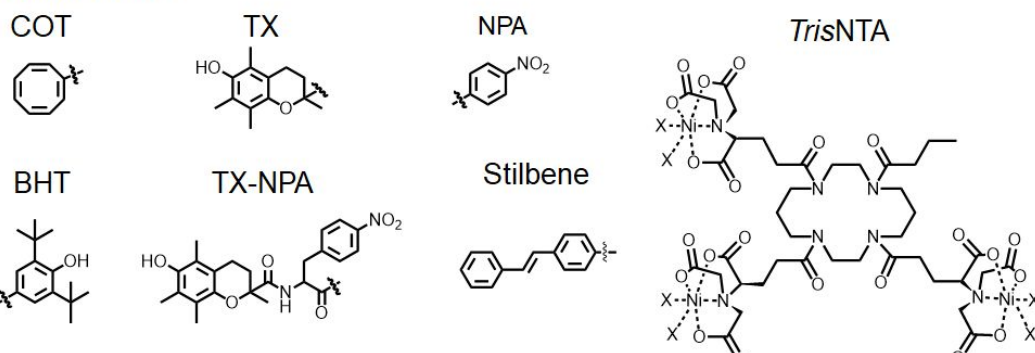
1
2
3
4
5
6
7
8
9
10
11
12
13
14
15
16
17
18
19
20
21
22
23
24
25
26
27
28
29
30
31
32
33
34
35
36
37
38
39
40
41
42
43
44
45
46
47
48
49
50
51
52
53
54
55
56
57
58
59
60
173 comprising TX and NPA³² (Figure 5b).

174 Three successful combinations of dye and photostabilizer were Cy5-COT (Figure
175 4d),²² Cy5-iROXS (Figure 4e),³² and *tris*NTA-Pro₄-Alexa647 (Figure 4f).³⁰ The
176 structures of COT, the iROXS compound TX-NPA and *tris*-NTA are depicted in
177 Figure 5. In these constructs the obtained total photon output of the self-healing dyes
178 are comparable or even higher (Cy5-COT) compared to the solution-based
179 photostabilization agents in buffer solution. Furthermore, all provided photophysical
180 parameters of individual fluorophores (e.g., brightness and signal-to-noise ratio) were
181 found to be improved, as indicated by the total photon count (see Figure 4, lower
182 panel). While such a super photophysical/chemical behavior is desirable, the
183 performance of the dye-stabilizer combination shown in Figure 4 is rather the
184 exception than what is commonly seen with most self-healing dyes.

a Fluorescent dyes



b Photostabilizers



185
186 **Figure 5.** Structures of fluorescent dye classes (a) and photostabilizers (b) that are established building
187 blocks of self-healing fluorophores. Displayed examples for corresponding dye classes: TMR for
188 Rhodamines, sulfo-Cy5 for Cyanines, ATTO647N for Carbopyronines, ATTO655 for Oxazines, Bophy

1
2
3 189 and Fluorescein.
4
5 190
6
7 191 Conjugation strategies of self-healing dyes
8
9 192 Thus far, three conceptually distinct approaches have been introduced to obtain high
10 193 local concentrations of photostabilizer around the fluorophores. Life science
11 194 applications require the simultaneous conjugation of a self-healing fluorophore, i.e.,
12 195 dye F and photostabilizer P, to a biomolecule B (Figure 6). In the seminal papers,
13 196 Lüttke used conjugation of dye and photostabilizer without further tethering to any
14 197 biological or chemical target. Blanchard and co-workers used *bis-N*-
15 198 hydroxysuccinimidylester-modified cyanine fluorophores for simultaneous coupling of
16 199 photostabilizer and biomolecules such as DNA, proteins and antibodies (Figure
17 200 6a).^{22,46} They also established a simpler, yet less general approach, which uses the
18 201 proximity of photostabilizer and fluorophore in double-stranded DNA constructs,
19 202 where covalent attachment of dyes was achieved via standard DNA-coupling
20 203 chemistry and proximity between P/F results as a consequence of DNA hybridization
21 204 (Figure 6b).^{22,24,33} The Cordes lab later established a versatile bio-conjugation
22 205 approach through the use of an unnatural amino acid scaffold (Figure 6c), where the
23 206 photostabilizer acts as a bridge between dye and biomolecule.¹⁹ This scaffold allows
24 207 the use of any combination of fluorophore, photostabilizer and biological target
25 208 (Figure 6c) and provided the first experimental evidence that self-healing can be
26 209 applied to various dye classes. Recently, Cosa and co-workers established *trisNTA*-
27 210 fluorophore complexes as parts of self-healing dyes by combining both the specific
28 211 polyhistidine tag (His-Tag) and photostabilizing properties of Ni²⁺ (Figure 6c, iii).³⁰
29
30
31
32
33
34
35
36
37
38
39
40
41
42
43
44
45
46
47
48
49
50
51
52
53
54
55
56
57
58
59
60

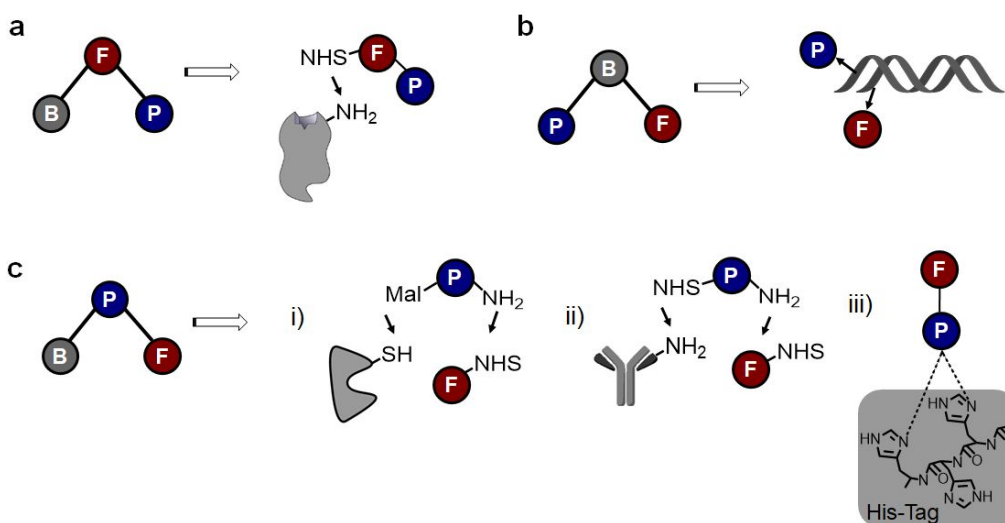


Figure 6. Conjugation approaches for self-healing dyes on biomolecular targets. (a) The dopamine receptor D2, (b) double stranded DNA, (c) proteins, antibodies and affinity-tags. Biomolecular target, photostabilizer and fluorophore moieties are denoted as B, P, and F, respectively.

In this manuscript, we refer to a fluorophore that is covalently linked to a photostabilizer (as shown in Figures 6a and 6c) as “directly linked,” i.e., the linkage of dye and stabilizer to two distinct biomolecules and self-assembly to induce proximity of fluorophore and stabilizer (as shown in Figure 6b) is referred to as “proximal-linkage.” It is important to note that a direct linkage of self-healing dyes so far requires complex synthesis of reactive precursors for biolabelling, something that still limits the applicability of the conjugates (see discussion section).

3. Current mechanistic understanding of intramolecular triplet-state quenching and photostabilization

In contrast to intermolecular approaches, intramolecular photostabilization does not rely on a large reservoir of stabilization agents (Figure 1). Instead, quenching of the triplet-state via energy transfer or PET is promoted by a high local concentration of one photostabilizer molecule.^{22,25,29,31} Thus, successful self-healing relies on the (chemical) stability of both fluorophore and photostabilizer under specific experimental conditions and the ability of the stabilizer to conduct many consecutive

1
2
3
4 235 healing cycles (Figure 7).

5 236 In the case of self-healing dyes with redox-active agents such as TX or NPA
6 (Figure 7a) the generated triplet state is quenched via collisions with the stabilizer
7 resulting in PET (Figure 7c).^{18,22,29,34} This process is similar to the mechanism of the
8 reducing-oxidizing photostabilization scheme (ROXS), where subsequent
9 complementary redox-reactions of solution stabilizers recover the electronic ground
10 state of the fluorophore. While for ROXS either radical-anion or cation are formed by
11 diffusion-based collision with different photostabilizers (Figure 1a), in self-healing the
12 same photostabilizer has to undergo two subsequent redox reactions. Initially it
13 seemed surprising that a single stabilizer can undergo multiple rounds of
14 photostabilization without loss of function.^{21,28}

15 246 For self-healing at first a charged biradical intermediate with triplet character
16 (Figure 6a,c) is formed.³⁴ The formation of the biradical is solvent dependent.⁴⁷⁻⁴⁸ In
17 support of this, Cy5-TX showed no triplet quenching in TAS studies in acetonitrile.^{23,31}
18 Furthermore, bulk photobleaching studies showed the solvent-dependency of the
19 photostabilizing effect of Cy5-NBA and Cy5-TX in acetonitrile and aqueous solutions,
20 respectively.³⁸ It is also important to note that, in contrast to intermolecular
21 stabilization, the newly formed biradical persists until subsequent reverse intersystem
22 crossing (k_{isc}) and back electron transfer (geminate recombination, rate k_{gr})
23 occurs.^{34,49} A process competing with photostabilization via geminate recombination
24 is separation of the photostabilizer and fluorophore biradical, i.e., separation of the
25 two radical centers resulting in the formation of two non-correlated radicals with
26 unrelated spin states (not shown in Figure 7a).⁹⁹ Successful recovery of the
27 fluorophore singlet state via intramolecular PET quenchers thus requires an efficient
28 intersystem crossing of the biradical intermediate with subsequent geminate
29 recombination (Figure 7a). In PET-based self-healing dyes, the chemical nature of
30 the photostabilizer, i.e., the redox-potential, is expected to have a large impact on the
31 photostabilization efficiency. Single-molecule studies as well as molecular dynamic
32 simulations suggest, however, that collision rates and the molecular interactions
33 governed by the biochemical environment are at least equally important for the self-
34

healing process (see discussion below).¹⁸

266

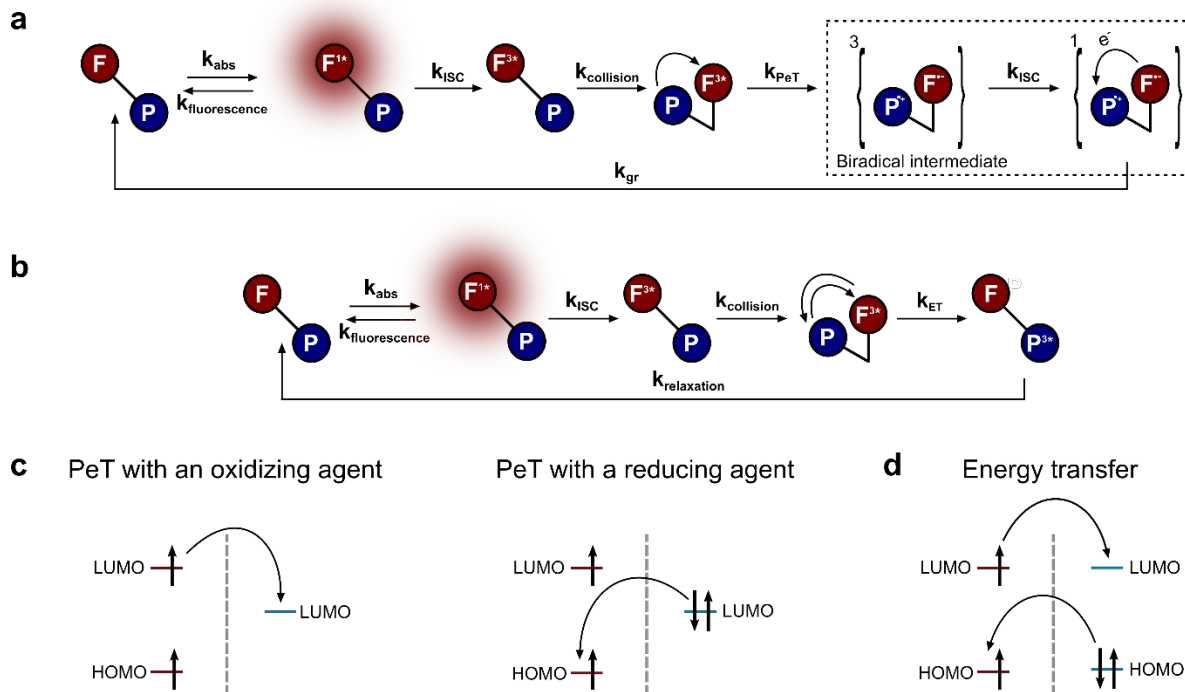


Figure 7. Photostabilization mechanisms (a, b) and energy-diagrams (c, d) of self-healing fluorophores with intramolecular PET (a, c) and triplet-triplet energy transfer processes (b and d). k_{abs} , rate of photon absorption; $k_{\text{fluorescence}}$, rate of emitting a photon through fluorescence; k_{ISC} , intersystem crossing rate; $k_{\text{collision}}$, collision rate; k_{PeT} rate of photoinduced electron transfer; k_{gr} , geminate recombination rate; k_{ET} , rate of energy transfer

In contrast to redox-active conjugates, photostabilization by physical triplet-state-

quenchers such as COT and Ni^{2+} (Figure 7b) proceeds through a physical mechanism without formation of charge-separated intermediates (Figure 7d). For an efficient photostabilization via this energy transfer, the photostabilizer should have a triplet state with lower (or equal) energy compared to that of the fluorophore (Figure 7d)⁵⁰. In COT this triplet-triplet energy transfer requires a planarization of the ‘boat-shaped’ COT, which leads to molecular relaxation and lowering of its triplet-state, allowing for quenching of fluorophore triplet-states with energies as low as 0.8 eV (Figure 7b, k_{ET}).⁵¹ Triplet-triplet energy transfer, however, becomes inefficient for large energy gaps between the triplet-states of photostabilizer (acceptor) and fluorophore (donor) explaining the poor performance of COT for certain dye classes,

1
2
3 285 e.g., fluoresceins.³³ A similar behavior has been observed for Ni²⁺, which works
4 286 through a different energy transfer mechanism.¹³ Additionally, the resulting sensitized
5 287 photostabilizer triplet state should be short-lived for efficient self-healing, i.e., it
6 288 should be available as a triplet-acceptor as soon as possible after energy transfer. In
7 289 COT, the triplet-state lifetime is on the order of ~100 μs,⁵² which allows for a fast
8 290 relaxation and recovery of the photostabilizer as triplet-acceptor (Figure 6b, k_{relaxation}).

9
10 291 A final point of importance is that high (local) concentrations of photostabilizers
11 292 can cause singlet quenching decreasing the fluorescence quantum yield of the
12 293 dye.^{24,30} Therefore, care has to be taken in linker design to optimize the collision rate
13 294 and geometrical orientation between fluorophore and photostabilizer. The overall
14 295 goal is to achieve efficient triplet quenching in combination with low singlet
15 296 quenching. This should also be taken into account for physical triplet-state-
16 297 quenchers, such as Ni²⁺,^{12-13,30} that can potentially quench singlet excited state by
17 298 enhanced ISC and increased formation efficiency of triplet-states. Again, the high
18 299 lying singlet excited state of COT, minimizes singlet state quenching due to energetic
20 300 mismatch with most fluorophores.³¹

21
22
23
24
25
26
27
28
29
30 301
31 302 Optimization strategies of photostability in self-healing dyes

32
33 303 In many cases, the photostability of self-healing dyes was found to be lower than that
34 304 of the pristine dye in photostabilizing buffer.^{14,19,25,33} Reasons for this can be low
35 305 (chemical) stability of the photostabilizer, generation of fluorophore radicals as
36 306 intermediates, the requirement of the stabilizer to efficiently undergo intersystem
37 307 crossing and a non-optimal collision rate between healer and fluorophore that does
38 308 not favor triplet- over singlet-quenching.

39
40 309 One key parameter for optimization of self-healing fluorophores is the collision
41 310 frequency and contact time between fluorophore/photostabilizer that can be tuned via
42 311 the linker length and linking chemistry on the specific biomolecule.³⁰⁻³¹ This was
43 312 already supported by the early data of Lüttke^{25,26} and Schäfer.⁹⁸ Blanchard and co-
44 313 workers provided additional DNA-based ruler experiments that supported the strong
45 314 distance-dependence of self-healing.²² While this relation followed the qualitative

1
2
3
4 315 trend expected for energy transfer processes (the closer the better), they also
5 316 demonstrated that there is an optimal linker length at short distances.³¹ At short
6 317 distances of course other interactions may become relevant too and might impact the
7 318 final performance of the self-healing dye. In selected cases for Cy5 conjugation to
8 319 COT maximized photostability also correlated with the shortening of triplet state
9 320 lifetimes and thus photostabilization efficiency increased monotonously with
10 321 decreasing linker length.³¹

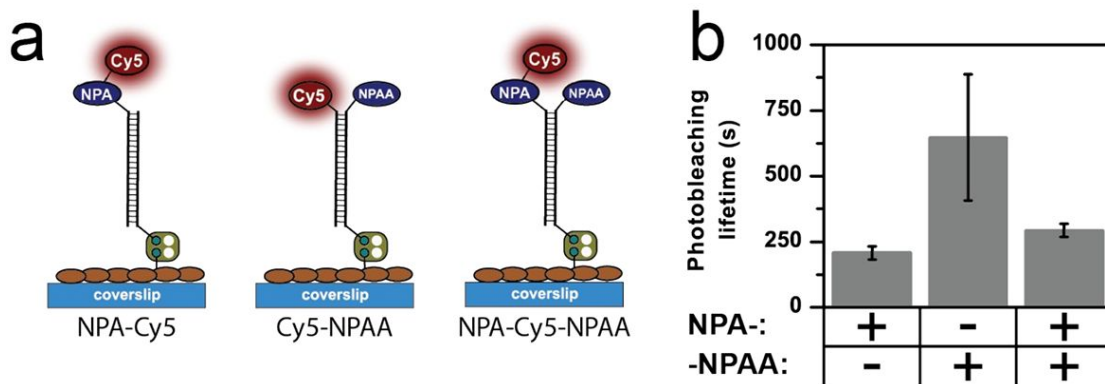
11
12
13
14
15
16
17 322 The crucial role of the linker length and geometry was also used by Cosa and co-
18 323 workers for optimization of self-healing Alexa647-*trisNTA* constructs.³⁰ Here, even
19 324 the nature of the linker was crucial for minimizing singlet excited state quenching by
20 325 Ni²⁺ while maintaining an efficient quenching of the triplet-state. A direct coupling of
21 326 fluorophores to *trisNTA* moiety containing three Ni²⁺ ions, resulted in fluorescence
22 327 quenching and only moderate improvement in photostability. Coupling to a rigid and
23 328 rather long Pro₁₂ linker prevented this unwanted quenching, however, it also reduced
24 329 the triplet-state quenching resulting in almost no effect of *trisNTA* group on
25 330 photostability of Alexa647. The best photostabilization was obtained when utilizing a
26 331 rigid and short Pro₄ linker allowing for even slightly better photostabilization efficiency
27 332 than solution-based photostabilization by Ni²⁺ (Figure 4f).³⁰ In a previous study,
28 333 Wagner et al. investigated the dependence of intramolecular triplet-triplet energy
29 334 transfer rates between a triplet donor and acceptor both based on collisions and
30 335 through a through-bond energy transfer⁵³. At very short bond lengths of less than
31 336 three carbon atoms, a through-bond energy transfer was detected. Strikingly, the
32 337 corresponding energy transfer rate was at least one order of magnitude higher
33 338 compared to the compounds with longer linker-lengths, in which diffusive collisions
34 339 dominate energy transfer rate. The information gained from this study may be helpful
35 340 for the future design of self-healing dyes with physical triplet state quenchers
36 341 featuring improved triplet quenching rates. The linker-length dependency of energy
37 342 transfer in Wagner et al. does, however, not match data shown by Zheng et al.³¹ on
38 343 Cy5-COT-self healing compounds with varying linker-length, suggesting a more
39 344 complex mechanism.

1
2
3 345 Another straightforward idea to improve photophysical dye properties, which was
4 346 only tested recently by the Cordes lab,¹⁴ is the combination of inter- and
5 347 intramolecular approaches. The idea was to either quench reactive fluorophore
6 348 states, which the intramolecular photostabilizer cannot recover, via intermolecular
7 349 pathways or to support the photostabilizer in its function directly. While there is no
8 350 strong evidence that photostabilizer destruction is a dominant reaction pathway,^{14,54}
9 351 redox-blinking (i.e., radical formation) was identified as one major problem of
10 352 intramolecular stabilization with physical quenchers such as Ni²⁺ and COT. The latter
11 353 manifests itself as ON- or OFF-blanks in otherwise stable single-molecule traces (see
12 354 data below).^{13,33}

13
14 355 In this study it was shown that solution photostabilizers had little to no effect on
15 356 the photostability of self-healing dyes.¹⁴ Mechanistically, this could be explained by
16 357 the idea that the intramolecular photostabilizer could outcompete the intermolecular
17 358 stabilizers on the basis of high local concentration.¹⁴ The tested compounds included
18 359 NPA conjugates (NPA-ATTO647N, NPA-Alexa555, NPA-Cy5) as well as proximal
19 360 Cy5-COT. Compounds were benchmarked against the effects of 2 mM TX or 2 mM
20 361 COT in solution, respectively. While there was an increase in count rate for NPA-
21 362 Atto647N with TX in solution, as well as to NPA-Alexa555 with TX or COT in solution
22 363 compared to the self-healing compound without stabilization agent, the overall trend
23 364 suggested only minor positive effects of photostabilization when solution additives
24 365 are present in addition to self-healing dyes.¹⁴

25
26 366 The Cordes lab also tried the use of multiple intramolecular stabilizers for self-
27 367 healing dyes. They used a proximally-stabilized Cy5 dye with a photostabilizer
28 368 consisting of both an oxidizing and a reducing agent (iROXS), which provided two
29 369 complementary redox-pathways for triplet- and radical-quenching.³² The origin of the
30 370 high photostability of proximal Cy5-iROXS (Figure 4c) was, however, not based on
31 371 two synergistic stabilizers, but was dominated by the linking geometry and contact
32 372 rates between Cy5 and NPA in these constructs. The second stabilizer TX had little
33 373 effect on the overall photostability of the dye. Smit et al. more recently tested a
34 374 combination of similar photostabilizers based on nitrophenylgroups (direct linkage of

1
2
3
4
5
6
375 NPA and proximal NPAA), which did also not result in higher photostability than
376 observed for a single photostabilizer as seen in Figure 8.¹⁴



20
21
22
23
24
378 **Figure 8:** Comparison of Cy5 photostability with different geometries of intramolecular photostabilization
379 by NPA and a combination of both. Reprinted from ref.¹⁴ with permission.

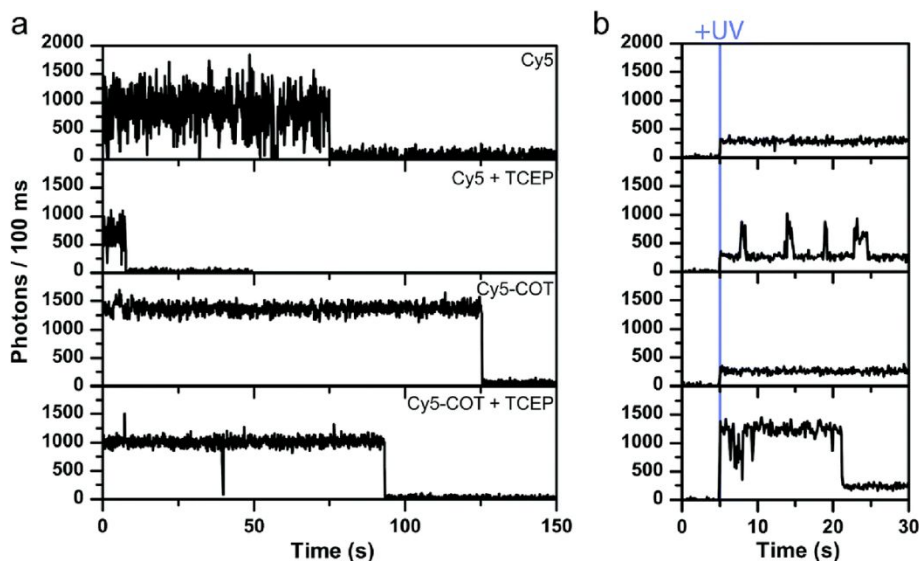
25
26
27
28
29
30
31
32
33
34
35
380
381 Interestingly, the Blanchard lab showed an increased photostability of Cy5 upon
382 linkage to two (instead of one) COT moieties.³¹ While the average counts before
383 photobleaching could be increased by coupling two COT molecules to Cy5, the
384 mechanistic origin of this gain remains unclear due to possible convolution of thiol-
385 induced photoswitching and self-healing processes in the characterization
386 experiments of these double-COT conjugates (see next section).

387
388 Competing pathways: Photostabilization vs. photoswitching

40
41
42
43
44
45
46
47
48
49
50
51
52
53
54
55
56
57
58
59
389 Self-healing dyes are commonly characterized and used in biological imaging
390 applications *in vitro* and *in vivo* or for single-molecule spectroscopy. In such
391 experiments they become exposed to varying biochemical conditions, which can
392 impact their function and photophysical properties (Figure 9). Examples of molecules
393 that largely impact dyes are reductive agents such as β -mercaptoethanol (BME),
394 mercaptoethylamine (MEA), glutathione, DTT or TCEP and molecular oxygen.⁵⁵⁻⁵⁶
395 All of the latter can be present up to millimolar concentrations *in vitro* (e.g., for
396 stabilizing proteins or components in a buffer) or are encountered naturally *in vivo*. In
397 STORM-type super-resolution microscopy similar compounds are even used at
398 higher concentrations (BME (143 mM), MEA (50 mM), TCEP (25 mM))^{57-61,108} to
399 reversibly switch fluorophores between bright and dark-states for single-molecule

1
2
3 400 localization and by that facilitate the reconstruction of images with a resolution
4 401 beyond the diffraction limit.

5
6
7 402 The Cordes lab recently investigated the interplay between inter- and
8 403 intramolecular processes in self-healing dyes both for photostabilizing (see previous
9 404 section) and photoswitching compounds.¹⁴ It became apparent that reducing agents
10 405 used for photoswitching in STORM microscopy induce fast “apparent”
11 406 photobleaching already in the presence of low reducer concentrations, e.g., 0.2 mM
12 407 TCEP (Figure 9a) or 5 mM MEA.³⁵ This effect was found to be most prominent for
13 408 cyanine fluorophores and was less pronounced for rhodamines and carbopyronines.
14
15 409 In detail the reversible OFF-switching caused by reductive agents such as TCEP
16 410 (see Cy5 in Figure 9a/b +UV) was much less efficient compared to Cy5-dyes with
17 411 proximal COT (see Cy5-COT in Figure 9a/b +UV).



412
413 **Figure 9.** Single-molecule fluorescence transients before (a) and after (b) UV irradiation of parent Cy5
414 fluorophore as well as Cy5-COT conjugates in the presence and absence of low TCEP concentrations
415 of 0.2 mM. Reprinted from ref.¹⁴ with permission. In the absence of TCEP (first and third panels)
416 fluorophores photobleach under continuous red excitation (a) but cannot be reactivated (b). In the
417 presence of TCEP apparent photobleaching is fast (due to photoswitching) and molecules can be
418 reactivated via UV radiation. The background increase in all panels in (b) is due to 375 nm excitation.
419 Copyright 2019 Royal Society of Chemistry.

420
421 ATTO647N showed no significant perturbation in terms of apparent
422 photobleaching time, whereas Alexa 555 showed an approximately two-fold
423 decrease in apparent photobleaching time with 200 μ M TCEP in solution. Here, the

1
2
3 424 effect was strongly reduced after NPA conjugation and on-times were almost as long
4 425 for the self-healing ATTO647N dye as for the parent dye with solution-based
5 426 stabilization. On Cy5 however, the effect on apparent photobleaching time was a lot
6 427 more prominent, as it decreased more than ten-fold under addition of 200 μ M TCEP
7 428 on the parent fluorophore, which mostly mitigated during solution based or
8 429 intramolecular stabilization. In our view the differing influence of TCEP is based on
9 430 the fact that only cyanines with methine chains ≥ 5 react efficiently,⁵⁸ whereas Cy3B
10 431 seems to be more susceptible to thiol-induced photoswitching or caging via sodium
11 432 borohydride rather than with TCEP.⁶²

12
13 433 We suggest that in self-healing dyes the conjugated photostabilizer efficiently
14 434 competes with the photoswitching agent (in the buffer) due to its high local
15 435 concentration in a “first-come first-quench” manner. This has important
16 436 consequences especially for cyanine dyes. It implies that photoswitching, which is
17 437 the basis for STORM super-resolution microscopy, occurs at least to some extent via
18 438 excited fluorophore states, since OFF-switching was shown to be photo-induced
19 439 (Figure 9). We also showed that intramolecular photostabilizers strongly influence
20 440 photoswitching kinetics. Thus the composition of photoswitching buffers have to be
21 441 adapted when self-healing dyes are used in localization-based super-resolution
22 442 microscopy.³⁵

23
24 443 Additionally, photoswitching agents are problematic components of imaging
25 444 buffers in characterization experiments of self-healing cyanine dyes, whereas other
26 445 classes are less susceptible to reactions with TCEP, MEA or photoswitching agents
27 446 in general. For example, it was previously concluded that proximal conjugation of
28 447 COT to Cy5 dramatically enhances its photostability via intramolecular
29 448 photostabilization with respect to Cy5 with COT as a solution additive. When arriving
30 449 at this conclusion, the effect of BME, TCEP and MEA on the photostabilization
31 450 efficiency and the photoswitching behavior of Cy5 and Cy5-COT derivative was
32 451 neglected. In the light of these findings, the photostabilization efficiency of self-
33 452 healing dyes was often overestimated, since the pristine dye in photostabilizing buffer
34 453 showed fast apparent photobleaching (which is reversible). The positive effect of an

1
2
3 454 intramolecular stabilizer on dye stability and properties persists, but might be
4 455 influenced slightly by the solution stabilizers. Thus various mechanistic studies of
5 456 self-healing dye in TCEP or thiol-containing buffers, especially those on cyanine
6 457 fluorophores, have to be evaluated critically and possibly revisited.
7
8
9
10

11 458 To the best of our knowledge, there are so far only three published mechanistic
12 459 studies on the photophysical properties of self-healing fluorophores that were
13 460 conducted in the absence of any intermolecular effectors such as oxygen and
14 461 reducing agents.^{14,30,35} Smit and van der Velde *et al.* screened a variety of
15 462 fluorophores directly conjugated to NPA, as well as Cy5 proximally-conjugated to
16 463 COT. The experiments showed a significantly higher photostability, signal stability
17 464 and brightness for all combinations compared to the native fluorophore. The
18 465 improvement could, however, not reach that acquired from intermolecular
19 466 stabilization of the native fluorophore through 2 mM TX or 2 mM COT.¹⁴ In another
20 467 study, Glembockyte *et al.* reported a highly photostable *trisNTA-Alexa647* self-
21 468 healing construct (Figure 5b), which showed a superior photostability when
22 469 compared to intermolecular stabilization with the same stabilizer (Ni^{2+} , Figure 4f).³⁰
23
24
25
26
27
28
29
30
31
32
33
34
35
36
37
38
39
40
41
42
43
44
45
46
47
48
49
50
51
52
53
54
55
56
57
58
59
60

470 471 Self-healing dyes and molecular oxygen:

472 Oxygen-dependent processes were so far studied only to some extent in the context
473 of self-healing dyes.^{22,31,38} Most experiments were conducted in the absence of
474 oxygen to avoid convolving effects. Since oxygen can promote a complex network of
475 primary and secondary photodamage pathways,³⁸ we will here only focus on the
476 fundamental question whether the intramolecular triplet state-quenchers, which are
477 present in self-healing dyes, can “outcompete” molecular oxygen. The mechanistic
478 idea would be to disable the action of oxygen by providing an intramolecular reaction
479 partner – as was observed in the competition of intramolecular and intermolecular
480 photostabilization and photoswitching, respectively (see previous sections).¹⁴

481 So far the self-healing dyes were shown to be rather ineffective in the presence of
482 molecular oxygen with quite moderate photophysical properties. In one study, the
483 same self-healing dye in the absence and presence of oxygen exhibited at least one-

1
2
3 484 to two orders of magnitude loss of total photon count.²² Blanchard and co-workers
4 485 had success in modifying the chemical nature of COT by electron-withdrawing
5 486 groups and with that could increase the performance of self-healing cyanine and
6 487 silicon-rhodamine fluorophores,³¹ yet the large discrepancy between the performance
7 488 of self-healing dyes with and without oxygen is not yet solved.

8 489 As intermolecular pathways compete with intramolecular processes (see
9 490 previous sections), one aspect causing this poor performance of self-healing dyes
10 491 might be that oxygen is always faster compared to triplet-quenching via
11 492 intramolecular stabilizers. Thus intramolecular triplet state quenching has not yet
12 493 overcome the diffusional speed limit. For oxygen we consider the diffusion limited
13 494 rate of quenching by molecular oxygen to be $10^{10} \text{ M}^{-1} \text{ s}^{-1}$ and the concentration of
14 495 molecular oxygen in solution of roughly $\sim 0.5 \text{ mM}$.⁶³ This suggests quenching rates of
15 496 $\sim 10^6 \text{ s}^{-1}$ for oxygen, which need to be overcome by competing intramolecular
16 497 photostabilizer. The upper limit of intermolecular triplet quenching in solution by
17 498 stabilizers such as Azobenzene⁶⁴ was experimentally determined to range from 10^7 -
18 499 $10^9 \text{ M}^{-1} \text{ s}^{-1}$. Assuming a similar reaction speed for COT, this suggests quenching
19 500 rates between $10^4\text{-}10^6 \text{ s}^{-1}$ for 1 mM COT solutions. While these rates are comparable
20 501 to those estimated with molecular oxygen, they certainly do not exceed them
21 502 supporting the experimental findings of rather unstable fluorophores in the presence
22 503 of oxygen even when using COT. The kinetic explanation for the poor performance of
23 504 COT given here is based on intermolecular reactions, but not intramolecular ones. To
24 505 quantitatively assess intramolecular effects, effective concentrations have to
25 506 calculated. These could be based on molecular dynamics simulations and can reach
26 507 values much higher than 1 mM. In that respect we are still missing key pieces in our
27 508 understanding that have to be obtained from further systematic studies in which
28 509 correlation between photostability and effective local concentrations of photostabilizer
29 510 have to be made rather than considering distances between photostabilizer and
30 511 fluorophore.

31 512
32 513 Impact of biological structures on self-healing dyes

1
2
3 514 DNA has become a well-established model system for characterization of fluorophore
4 515 photophysics in general, especially when working with single-molecule techniques. In
5 516 self-healing dyes with proximally-linked photostabilizers on a DNA scaffold, the effect
6 517 of DNA itself on the photophysical properties of the dye cannot be neglected and
7 518 other less perturbing systems such as rigid poly-proline motifs^{14,19,22,30} might be
8 519 preferable for future studies. DNA can influence the photophysics of dyes via a
9 520 number of different mechanisms reported in the literature.⁶⁵⁻⁶⁷ First, the DNA base
10 521 guanine is an electron donor, which can quench the fluorescence of dyes with low
11 522 reduction potentials, e.g., oxazines and rhodamines that become reduced easily via
12 523 PET.⁶⁷⁻⁷⁰ This can, in turn, decrease the brightness of these fluorophores and cause
13 524 redox blinking when attached in close proximity to guanine or, in particular, when
14 525 attached close to guanine repeat sequences.⁶⁷ That being said, the electron donating
15 526 ability of guanine could also potentially influence the lifetimes of radical species of
16 527 fluorophore that are formed via other pathways, e.g., photooxidation.

17 528 Another important interaction possibility of dyes with DNA is stacking of the dyes
18 529 to the end-bases as well as binding to major and minor grooves of the DNA duplex,⁶⁵⁻
19 530 ^{66,71-72} which can influence the rate and efficiency of photostabilization in self-healing
20 531 dyes. This was shown for terminal attachment of dyes in direct conjugation to a
21 532 nitrophenyl-group and in proximity, which likely resulted in completely distinct
22 533 photophysical properties of the dye due to different interactions with the DNA.¹⁸

23 534 The effect of DNA duplex on photophysical properties and photostabilization
24 535 efficiency of a common cyanine dye Cy5 is illustrated in Figure 10 by yet unpublished
25 536 data from the Cosa lab. Here, the dye was attached to two distinct DNA duplexes
26 537 (see Table S1 for ssDNA sequences) and its photostability was evaluated in the
27 538 presence of photophysical (0.4 mM Ni²⁺) and photochemical (ROXS consisting of 1
28 539 mM AA and 1 mM MV²⁺) photostabilizers in solution. Figure 10a contains single-
29 540 molecule fluorescence trajectories obtained for the duplexes in the presence of Ni²⁺.
30 541 Under these conditions, the triplet-states are expected to be efficiently quenched by
31 542 Ni²⁺, therefore, any blinking that is observed in single-molecule fluorescence
32 543 trajectories is attributed to the formation of long-lived radical species, which are not

observed in the presence of ROXS. Cy5-DNA duplex 1 (Figure 10, left panel) displayed a large extent of redox blinking and, in turn, less efficient photostabilization by Ni^{2+} when compared to photochemical stabilization by ROXS system capable of scavenging reactive radical intermediates (Figure 10b, left). On the other hand, the Cy5-DNA duplex 2 showed almost no redox associated blinking and, consequently, very comparable photostabilization efficiency by Ni^{2+} and ROXS. These findings illustrate a crucial role that DNA duplex can play on the photostabilization of dyes, suggesting either a DNA-induced radical formation (prominent in duplex 1) or possibly potential quenching of radicals induced via other pathways (e.g., photooxidation) by the DNA scaffold (prominent in duplex 2). Further mechanistic studies, e.g., of DNA sequence dependence on these processes, may help to shed light on the nature of these blinking events and the role of the DNA scaffold.

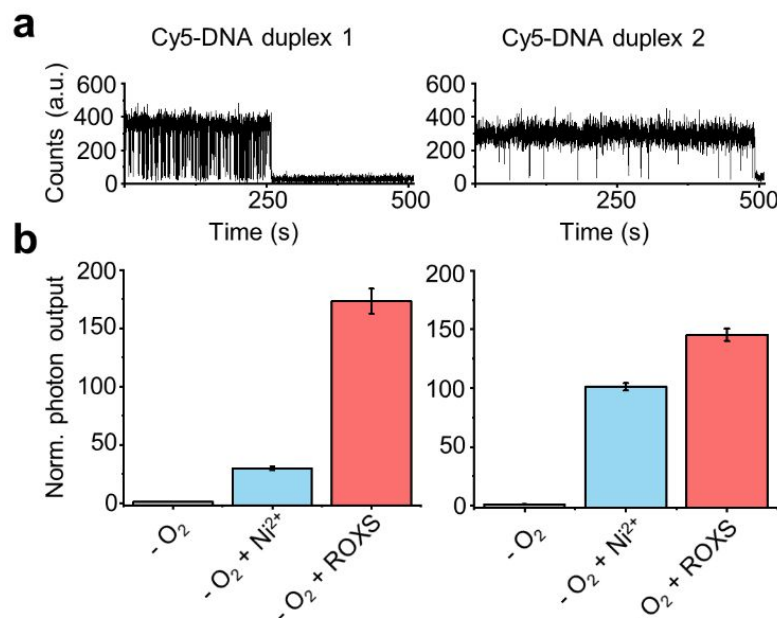


Figure 10. Effect of DNA duplex on the photophysical properties and photostabilization efficiency of Cy5. (a) Single molecule trajectories of Cy5 when attached to two different DNA duplexes (left and right) in the presence of enzymatic oxygen scavenger and 0.4 mM Ni^{2+} acquired at 100 ms time resolution. Under these conditions the triplet-state of Cy5 is efficiently quenched, therefore short blinking events that are observed correspond to different extent of radical formation; (b) Normalized photon outputs obtained for the two duplexes in the presence of photophysical (0.4 mM Ni^{2+}) and photochemical (ROXS consisting of 1 mM AA and 1 mM MV^{2+}) photostabilization approaches. Cy5-DNA duplex 1 shows that the high extent of redox blinking is photostabilized much more efficiently with the ROXS system. In contrast, for Cy5-DNA duplex 2 almost no redox blinking is observed and both photostabilization

1
2
3 567 approaches are comparable emphasizing a crucial role of DNA environment. A full description of
4 568 material and methods including additional experimental data is provided in Supplementary Note 1 and
5 569 Figure S1. Data from the Cosa lab.
6
7 570

8
9 571 Fewer studies of self-healing dyes have been done on biological scaffolds such
10 572 as proteins, antibodies or “neutral” scaffolds such as polyprolines.^{14,19,22,30} As for
11 573 DNA, the effect of the protein environment plays an important role in the
12 574 photophysics of the dye. Proteins present a challenging environment for prediction of
13 575 possible interactions of the dye/photostabilizer with charged/hydrophobic residues,
14 576 structural elements, flexible loops or chemically reactive sites such as cysteines.
15
16

17 577 A first step into a systematic characterization of interactions between (self-
18 578 healing) dyes and proteins was recently published.¹⁴ Here, ATTO647N and Cy5 were
19 579 not linked to a photostabilizer but conjugated to aromatic amino acids (Trp, Phe, Tyr).
20 580 Interestingly, Trp-ATTO647N and Trp-Cy5 showed barely any change in
21 581 photostability or signal quality compared to the pristine dyes in the absence of
22 582 oxygen and intermolecular photostabilizers. The addition of TX as intermolecular
23 583 photostabilizer, i.e., buffer additive, was much less effective in the presence of
24 584 covalently-coupled Trp. This suggests Trp can act similarly to NPA/COT via
25 585 intramolecular PET-processes as discussed above but inhibits the function of buffer
26 586 additives such as TX. In essence Trp creates a truly bad environment in that it does
27 587 not stabilize fluorophores by itself, yet it does not allow solution-photostabilizers such
28 588 as TX to interact with the dye either. Such interaction, however, was not observed
29 589 while using COT as a solution based stabilizing agent, suggesting the more effective
30 590 action of COT. Interestingly, other amino acids with lower tendency for reductive PET
31 591 (phenylalanine and tyrosine) had no notable effect on the photophysics of Cy5 and
32 592 ATTO647N.¹⁴ For applications in proteins, the effect of tryptophan (and other factors)
33 593 would now need to be studied in self-healing dyes to understand the full implications.
34
35

36 594
37 595 Impact of fluorescent labels on biological systems

38 596 Covalently linking a fluorophore to a photostabilizer does not only alter its
39 597 photophysical behaviour, but it also increases the size and molecular weight of

1
2
3 598 the compound to a large extent. While an increase in label size is one possible
4 599 problem, also changes of the chemical nature of the label have to be considered.
5
6 600 The introduction of hydrophobic groups via aromatic or aliphatic rings might alter
7 601 the interactions of the label with a biomacromolecule.²⁰

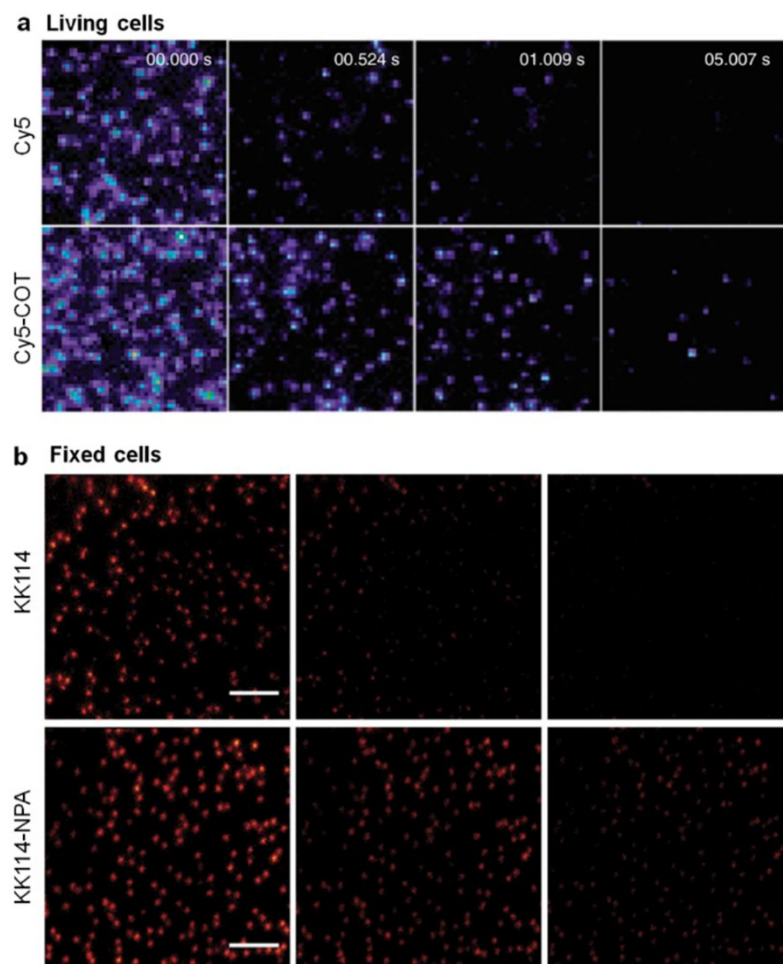
8
9
10 602 Only a limited number of studies were done to characterize such
11 603 perturbations of, e.g., paramagnetic spin-labels for EPR or fluorescent probes on
12 604 biological constructs such as DNA or proteins.⁷³ To the best of our knowledge,
13 605 there is no systematic investigation on the impact of self-healing dyes on, e.g.,
14 606 the biochemical behavior of proteins or DNA. Especially in studies with the aim is
15 607 to draw conclusions about the dynamic or structure of biological systems, care
16 608 has to be taken while selecting labeling position and compounds like in most
17 609 other labeling approaches. Control experiments such as K_d -estimation of labelled
18 610 proteins as presented in van der Velde et al. with self-healing dyes,¹⁹ are one
19 611 example for assessing the label influence. Sánchez-Rico et.al. presented a
20 612 comprehensive guideline for choosing fluorescent labels and labeling positions in
21 613 a way that minimize interference on protein function, which in our opinion should
22 614 also be taken into account during such investigations using self-healing dyes.⁷³
23
24 615 In combination with fluorescence-independent biochemical assays to ensure
25 616 functionality of the system under investigation, we expect assays with low
26 617 biological interference, especially since the molecular weight and size are still
27 618 much smaller than those of frequently used fluorescent proteins.

28
29
30 619
31
32 620 **4. Recent applications of self-healing dyes**
33
34 621 The self-healing approach could potentially improve the performance of fluorophores
35 622 in various imaging, spectroscopy and diagnostic applications. Recent examples of
36 623 their use include high resolution optical imaging (STED/STORM^{19,35}), single-molecule
37 624 FRET,^{19,25,46} near-Infrared photostable bioimaging,³⁷ super-long imaging-tracking of
38 625 single individual molecules,⁷⁴ life-cell imaging using self-healing dyes for
39 626 multichromophore probes⁷⁵ and tracking of submersible nanomachines.⁷⁶

40
41
42
43
44
45
46
47
48
49
50
51
52
53
54
55
56
57
58
59
60 627

628 Cellular imaging and high-resolution microscopy

629 In particular for cellular and super-resolution imaging, the available photon budget is
630 important and thus various photostabilization buffers have been tested in the field.⁷⁷
631 Blanchard's group demonstrated increased photobleaching lifetime of Cy5-COT
632 conjugates *in vivo* Chinese hamster ovary (CHO) cells compared to the parent
633 fluorophore using fluorescence imaging (Figure 11a).²²



634
635 **Figure 11.** (a) Single-molecule total internal reflection fluorescence image sequences of living CHO
636 cells containing dopamine D2 receptors labeled with Cy5 and Cy5-COT. Reprinted from Ref²² with
637 permission. Copyright Nature Publishing Group. (b) Repeated scanning of the same area of KK114 and
638 NPA-KK114 labeled fixed PtK2 cells in the STED mode. The figure was partially adapted from Van der
639 Velde *et al.*¹⁹

640
641 Applications of self-healing dyes in super-resolution imaging and live-cell
642 imaging were shown for stimulated emission depletion (STED) microscopy and
643 stochastic optical reconstruction microscopy (STORM).^{14,19,35} The Cordes group has

1
2
3
4 644 successfully shown a reduced fading of fluorescence from KK114-NPA conjugates
5 645 compared to the parent fluorophore as stains in the nuclear pore complex in fixed
6 646 mammalian PtK2 cells in STED imaging (Figure 11b).¹⁹ Recently, they also
7 647 demonstrated a significant increase in STED resolution from ATTO647N-NPA
8 648 conjugates compared to the parent fluorophore, resulting from highly improved
9 649 photophysical performance providing count-rates of individual molecules of up to 1
10 650 MHz without use of plasmonic effects.³⁵ So far self-healing dyes with increased
11 651 photostability have been able to demonstrate their potential for STED-type
12 652 microscopy, where the achievable resolution is determined by the increased number
13 653 of laser excitation cycles.⁵⁴ It remains to be shown, how much improvement can be
14 654 made via intramolecular photostabilization in STED in comparison (or combination)
15 655 with approaches such as protected STED⁷⁸ and Minflux.⁷⁹

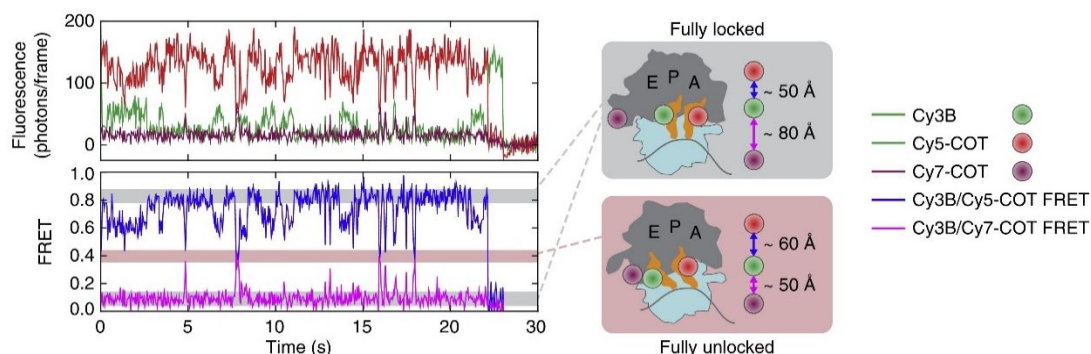
16
17 656 Applications of self-healing dyes in localization-based super-resolution
18 657 microscopy (STORM-type imaging) turned out to be more complicated as discussed
19 658 already in previous sections. STORM demands the fluorophores with on-off switching
20 659 property as well as good photostability.¹⁴ Since thiol derivatives (TCEP, BME or
21 660 MEA) are used as standard photoswitching agents to make the fluorophores cycle
22 661 between the on and off states,⁵⁷ yet the photoswitching agents are largely altered in
23 662 self-healing dyes.³⁵ Thus, more research efforts are required in order to lay out
24 663 general design rules for self-healing dyes capable of photoswitching and to enable
25 664 their widespread use in super-resolution imaging.

26
27 665
28
29 666 Single-molecule Förster resonance energy transfer

30
31 667 Single-molecule Förster resonance energy transfer (smFRET) is an emerging tool for
32 668 probing dynamics and interactions in biological systems both *in vivo* and *in vitro*.⁸⁰ In
33 669 these experiments, energy transfer is used as a molecular ruler to determine inter-
34 670 and intramolecular distances with the temporal resolution of spectroscopic
35 671 techniques down to nanoseconds.⁸⁰ Mapping dynamic biological processes presents
36 672 high demands on the brightness, signal stability and photobleaching lifetime of the
37 673 fluorescent probes involved.⁴⁶

1
2
3 674 The applicability of self-healing dyes for smFRET has already been
4 675 demonstrated for smTIRF microscopy^{25,46} and solution based alternating laser
5 676 excitation (ALEX) in confocal microscopy.¹⁹ Recently, Juette et al. demonstrated the
6 677 applicability of self-healing dyes in two and three color smFRET experiments on
7 678 ribosomal pre-translocation complexes.⁴⁶ Their two-color FRET experiments show
8 679 the versatility of the Cy3 and Cy5-COT fluorophore pair with distinct FRET states for
9 680 both high time-resolution (2ms), showing sub-second protein dynamics, as well as
10 681 low time resolution (500ms) visualizing protein dynamics that occur over tens of
11 682 minutes. Furthermore, in the same study, Cy3B, Cy5-COT and Cy7-COT were used
12 683 to monitor correlated movement inside the ribosomal pre-translocation complex
13 684 through three-color FRET (Figure 12). The time-traces demonstrate stable
14 685 fluorescence, illustrating the excellent fluorophore quality under multi-wavelength
15 686 excitation.^{46,81}

16
17
18 687 For solution-based ALEX experiments⁸² a clear increase in photostability of the
19 688 FRET pair Cy3B and NPA-ATTO647N compared to the non-stabilized pair Cy3B-
20 689 ATTO647N was observed under high irradiation conditions¹⁹ While the photostability
21 690 for this dye pair did not meet the level of solution-based stabilization conditions, the
22 691 increase in photostability compared to the parent fluorophore in absence of stabilizer
23 692 makes it still desirable in the situations described in section 1.



50
51 693 **Figure 12.** Multi-color smFRET with self-healing fluorophores. Ribosomal pre-translocation complexes
52 694 were labeled as shown (cartoon) on tRNA molecules and ribosomal protein L1 and imaged as described
53 695 previously.⁸³ Fluorescence (top) and FRET traces (bottom, defined here as acceptor fluorescence
54 696 divided by total fluorescence) of labeled pre-translocation complex imaged at 40 ms time resolution
55 697 during continuous laser excitation (120 mW, 532 nm wavelength). Reprinted from ref.⁴⁶ with permission.
56
57
58
59
60

1
2
3
4
5
6
7
8
9
10
11
12
13
14
15
16
17
18
19
20
21
22
23
24
25
26
27
28
29
30
31
32
33
34
35
36
37
38
39
40
41
42
43
44
45
46
47
48
49
50
51
52
53
54
55
56
57
58
59
60

699

700 Solution based photostabilization through ROXS is especially challenging for multi-
701 color FRET applications due to differences in fluorophore redox potentials. As a
702 general approach, self-healing could bypass this problem by using a stabilizing
703 moiety that is optimized for each fluorophore. The physical quencher COT has shown
704 an efficient photostabilizing effect for a wide range of fluorophores throughout the
705 visible spectrum, allowing it to be used for a variety of fluorophore pairs.³³ However,
706 the effect does not seem to be optimized for some selected fluorophores such as
707 fluoresceins or specific combinations of donor-acceptor dyes required for FRET,^{28,33}
708 leaving room for use of self-healing fluorophores with distinct and optimized
709 fluorophore-stabilizer combinations.

710

711 **5. Toward a next generation of self-healing dyes**

712 As is apparent from this review, self-healing dyes have become an attractive
713 alternative method for photostabilization since their introduction in the 1980s. Their
714 successful applications show possible positive impact on various research fields, yet
715 they still have to reach their full potential. In our view, there are three major directions
716 that require further attention to make the approach more mature and generally
717 applicable.

718

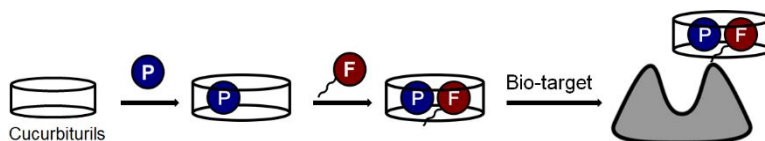
719 New stabilizers and strategies to further improve self-healing

720 When comparing the photostability of PET-based and energy transfer-based self-
721 healing dyes, the latter ones often show better performance. One possible
722 explanation for this is that in PET-based photostabilization with redox active triplet-
723 state-quenchers the reactive triplet biradical intermediate is a key bottleneck (Figure
724 7). Therefore, a possible approach to improve the performance of these dyes would
725 be to enhance the rate of ISC in this newly formed triplet biradical (i.e., reduce its
726 lifetime). Mechanistic transient absorption studies with Cy3B have evaluated the
727 ability of different reducing agents/triplet-state-quenchers (such as ascorbic acid, n-

1
2
3 728 propyl gallate, Trolox, and BME) to assist in ISC in the newly formed geminate
4 729 radical pair formed following PET. Studies involved comparing the extent of geminate
5 730 recombination versus radical escape from the geminate radical ion pair in solution.³⁴
6
7 731 Similar mechanistic approaches could be used to screen different redox active
8 732 photostabilizers to identify promising candidates for self-healing dyes capable of
9 733 enhancing the ISC rate via different interactions (e.g., spin orbit coupling or hyperfine
10 734 interactions). Given almost quantitative geminate recombination for thyil radical for
11 735 solution-based photostabilization with BME, thiol containing antioxidants could be of
12 736 potential interest. Furthermore, the lifetime of triplet biradical intermediate has been
13 737 shown to be quite sensitive to the length of the linker between the two radical
14 738 centers.

15
16 739 Several approaches have been reported to improve photophysical properties of
17 740 the fluorophores including by protein partner,⁸⁴⁻⁸⁵ through fluorination,⁸⁶⁻⁸⁷ and by
18 741 making dendrimers or nanoconjugates.^{75,88-90} For the self-healing mechanism, the
19 742 excited triplet-state quenching *via* Dexter-type energy transfer is considered to be
20 743 more efficient for various fluorophore scaffolds, since it has little impact on singlet
21 744 state quenching. The lower energy gap (labeled as ΔG in Figure 7d) between the
22 745 excited triplet-state and ground state of the photostabilizer imparts quicker rate of the
23 746 triplet-state quenching *via* Dexter-type energy transfer. From previous research, COT
24 747 has shown the significance to improve the fluorescence performance of the
25 748 conjugated fluorophores. COT-based derivatives with even more extended
26 749 conjugated π -system would have even lower ΔG and are predicted to largely
27 750 contribute to the energy transfer for triplet-state quenching. However, these
28 751 chemicals have poor solubility in water, which limits their further conjugation and
29 752 application. To solve this problem, we propose to utilize host-guest chemistry.⁹¹⁻⁹³
30
31 753 Cucurbiturils would be promising hosts for the complexation of organic guests, due to
32 754 their ability to internalize alkyl chains or cyclobenzenes within its hydrophobic cavity
33 755 formed by carbonyl groups.⁹¹ As illustrated in Figure 13, cucurbituril renders dual
34 756 ends and large enough cavities to encapsulate photostabilizers and fluorescent dyes
35 757 simultaneously and are known to improve dye brightness and photostability.⁹¹ The

1
2
3 758 assembled complex of cucurbiturils, photostabilizers and fluorophore is expected to
4 759 combine the biomolecules in need from the active site of fluorophores and have
5 760 excellent photophysical properties. This idea may explore the possibilities of other
6 761 dominant mechanisms for photostabilizing self-healing dyes.
7
8
9
10



16 763 **Figure 13.** Illustration scheme of host-guest complexation of cucurbiturils with fluorophores and
17 764 photostabilizers and their further conjugation to biomolecules.
18
19
20

21 765 An alternative approach to improve the photophysical properties of dyes is to
22 766 enhance their excitation and radiative rate *via* the help of plasmonic nanostructures,
23 767 such as noble metal nanoparticles.⁹⁴⁻⁹⁷ The increased radiative rate of dyes in the
24 768 vicinity of plasmonic nanostructures and, in particular, in the plasmonic hotspots,
25 769 reduces the time spent in the excited state and, hence, increases the total number of
26 770 fluorescence photons. One of the main difficulties in utilizing plasmonics for this
27 771 purpose is the challenge of achieving a precise and stoichiometric control of the
28 772 distance between the fluorophore and the plasmonic nanostructure. Nevertheless, in
29 773 recent years the DNA origami technique⁹⁷ has been elegantly exploited to circumvent
30 774 this challenge. For example, up to 30-fold increase in photon output have been
31 775 reported for dyes placed in the vicinity of nanoparticles.⁹⁷⁻⁹⁸ The combination of these
32 776 two approaches, i.e., plasmonics and photostabilization *via* self-healing approach
33 777 may prove extremely beneficial when maximizing the photon count rates that can be
34 778 achieved from a single fluorescent dye while enabling to study the conformational
35 779 changes of biomolecules on the time scales previously unattainable to typical single-
36 780 molecule fluorescence experiments.
37
38
39
40
41
42
43
44
45
46
47
48
49
50
51
52
53
54 782
55 783 Alternative fluorophores
56
57
58
59
60 784 When it comes to designing improved and even more robust self-healing
61 785 fluorophores, one could also envision testing fluorophores that possess superior
62 786 photophysical properties, such as low intersystem crossing yield, or optimized

1
2
3 787 fluorescence quantum yield (azetidine dyes developed by the Lavis group⁹⁹). One
4 788 could also combine the self-healing approach with other photostabilization strategies.
5
6 789 For example, fluorophore scaffold modifications with electron withdrawing
7 790 substituents (such as fluorine) has been shown to improve the photostability of
8 791 certain cyanine, rhodamine as well as coumarine dyes due to the reduced
9 792 susceptibility of fluorophores to reaction with singlet oxygen.^{84-87,100-102} Another type of
10 793 dye instability that is not discussed as often is their spectral instability
11 794 (photoswitching to dim or spectrally-shifted states).⁹⁸ An approach to overcome this
12 795 spectral instability in rhodamine class of dyes by covalent modification of their
13 796 scaffold has been recently proposed by the Hell group¹⁰³ and could be of potential
14 797 interest when designing even more optimized self-healing dyes for single-molecule
15 798 fluorescence experiments.

16
17 799 Another exciting question would be whether intramolecular photostabilization can
18 800 be used for fluorescent proteins (FP). A major hurdle to characterize FPs is a more
19 801 complex photophysical behavior, where not only the properties of the chromophore
20 802 but also other factors such as the protein barrel and specific environment will play a
21 803 huge role for the observed properties. Often complex photochemical reaction
22 804 pathways exist that might not render the triplet-state of FPs the main problem in their
23 805 photophysics. To test intramolecular photostabilization on FPs one fundamental
24 806 problem relates to how the photostabilizer could be introduced to the β -barrel of the
25 807 protein (Figure 14A). While certain unnatural amino-acids exist that provide a
26 808 nitrophenyl-group, the experimental realization of such a strategy will present
27 809 different challenges (protein expression levels, correct folding, etc.).

28
29 810 The Cordes lab has recently taken first steps towards testing GFP-variants
30 811 containing covalently-linked photostabilizers. For this a GFP double cysteine mutant
31 812 was labeled and analyzed with photostabilizer moieties in vicinity to the
32 813 chromophore, yet with no direct contact between the two (Figure 14A). This protein
33 814 was taken as a basis for external labelling of the GFP barrel with photostabilizer-
34 815 maleimides of TX, NPA, COT and azobenzene.¹⁰⁴

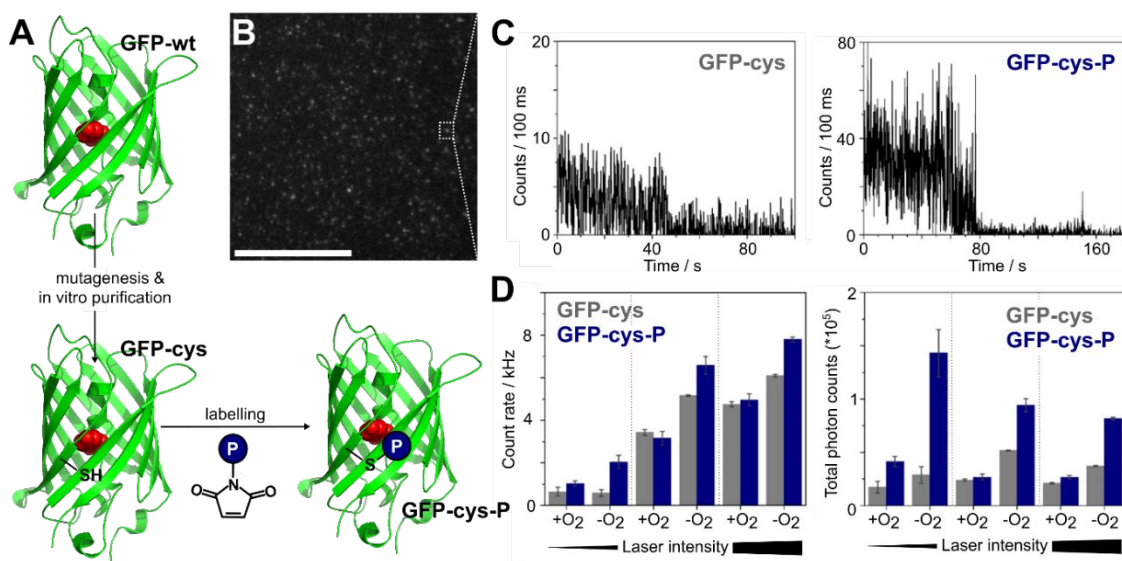


Figure 14. (A) Experimental strategy for the development of fluorescent proteins with covalently-linked photostabilizers outside the β -barrel via cysteine labelling using reactive photostabilizer derivatives P. (B-D) Fluorescence characterization of individual GFPs: (B) image with 10 μm scale bar and (C) single-molecule time traces of individual GFP. (D) Quantitative photophysical parameters of GFP in the presence and absence of covalently linked azobenzene; further parameters investigated were laser intensity (0.4, 2.0 and 3.2 kW/cm^2) and the presence and absence of molecular oxygen; data from ref. 104.

In this recent study, it could be shown that a mutant of alpha-GFP, mutant GFP-QC2 (C48S, A206C, L221C) features substantial increases in photostability (Figure 14C) upon conjugation of azobenzene to the two cysteines. Count-rate and total detected photon numbers were derived from TIRF movies of individual GFP molecules, using methods as reported previously, and showed that azobenzene can improve these properties up to 5-fold at intermediate laser excitation power, yet mostly in the absence of oxygen (Figure 14D). The effects were also not related to a change in redox-state of the two close-by cysteines (A206C, L221C) since labelling with other photostabilizer-maleimides did not have such an impact (Figure S2) and the GFP variant's fluorescence quantum yield was insensitive to presence of reducing agents. The mechanistic basis of the improvement could not yet be related directly to triplet-state quenching, however, the results supports the idea that also FPs might be in scope for the self-healing dye technology. This can even be done by rational choice of triplet-state quenchers based on recent reports on the triplet properties of FPs.¹⁰⁵

1
2
3 840 Alternative conjugation strategies

4
5 841 A remaining fundamental hurdle is to synthesize and characterize self-healing dyes
6
7 842 with appropriate reactive sites for various biomolecules while keeping the stabilizer at
8
9 843 the right distance. Blanchard and co-workers sell a selected number of self-healing
10
11 844 cyanine dyes (www.lumidynetechnologie.com). There is, however, no commercial
12
13 845 solution, which is generally applicable to all dyes and may allow commercial dyes to
14
15 846 be upgraded to a self-healing dye. As shown in Figure 5, self-healing dyes are
16
17 847 always pre-modified with the photostabilizer to allow bio-labelling. Although the
18
19 848 Cordes lab introduced a general approach using unnatural amino acid-based
20
21 849 photostabilizers to generate self-healing constructs, these are not commercially
22
23 850 available yet, require a demanding synthesis procedure and consume large amounts
24
25 851 of expensive commercial dyes during preparation. Even the proximity of
26
27 852 photostabilizers to the fluorophores through DNA hybridization can reduce the
28
29 853 chemical synthesis to some extent, but has very limited applicability. We think, one
30
31 854 key step for advancement of self-healing dyes is an easy, universal, and modular
32
33 855 approach that transforms normal dyes into self-healing dyes once they bind the
34
35 856 biotarget. The procedure should be based on established linking chemistry (mostly
36
37 857 click chemistry) and should be integrated into existing protocols, thus, requiring only
38
39 858 commercially available fluorophores.

40
41 859 To address this problem, the Cordes lab is currently developing a class of
42
43 860 compounds that allow biolabelling of virtually any biomolecule *in vitro* with a
44
45 861 fluorophore of tunable properties. A bio-reactive site, photostabilizing moiety and tag
46
47 862 are linked together followed by a subsequent coupling of a fluorophore to the tag.
48
49 863 This subsequent fluorophore coupling step allows for even more flexibility for the
50
51 864 choice of fluorophores. Via the insertion of a linker-molecule before fluorescent
52
53 865 labelling, it would be possible to even alter other fluorophore properties and not only
54
55 866 increase photostability. Such functionality could include photoswitching capabilities,
56
57 867 additional purification tags, different hydrophilicity, or chemical sensing (Zhang,
58
59 868 Isselstein, Köhler, Eleftheriadis, Herrmann & Cordes, unpublished).
60
61 869

1
2
3
4
5
870

6. Conclusions

This Perspective summarized the current state of the art of self-healing dyes as new promising class of fluorescent labels. We provided details on their historical development, highlighted the established building blocks of self-healing dyes, mechanistic understanding and compared the performance to other photostabilization approaches. Besides a description of their most recent applications in high-resolution, live-cell and single-molecule imaging, we also detailed remaining key limitations: (i) How could mechanistic understanding further advance photostabilization efficiency of self-healing dyes especially accounting for different biochemical environments and the presence of molecular oxygen? (ii) What requirements do we have in term of bioconjugation for self-healing dyes? Finally, we showed new data that contributed towards solving these problems showing fluorophore redox-blinking in double-stranded DNA with differing base sequences and summarized a recently published study toward use of intramolecular photostabilization for fluorescent proteins.

886

Associated content

Supporting Information. Materials and methods and additional data for Figures 13 and 14.

890

Notes

The authors declare no competing financial interests.

893

Acknowledgments

This work was financed by Deutsche Forschungsgemeinschaft (SFB863, project A13; cluster of excellence CiPSM, LMUexcellent), an ERC Starting Grant (No. 638536 – SM-IMPORT to T.C.) and by the Center of Nanoscience Munich (CeNS). G.C. is grateful to the Natural Sciences and Engineering Research Council of

1
2
3 899 Canada (NSERC) and the Canadian Foundation for Innovation (CFI) for funding. L.
4 900 Zhang and V.G. thank the Alexander von Humboldt foundation for postdoctoral
5
6 901 research fellowships. T.C. thanks J.S. Cordes for his patience while writing this
7
8 902 manuscript.
9
10
11
12
13
14
15
16
17
18
19
20
21
22
23
24
25
26
27
28
29
30
31
32
33
34
35
36
37
38
39
40
41
42
43
44
45
46
47
48
49
50
51
52
53
54
55
56
57
58
59
60

References

1. Minoshima, M.; Kikuchi, K. Photostable and photoswitching fluorescent dyes for super-resolution
2 imaging. *J. Biol. Inorg. Chem.* **2017**, *22*, 639-652.
3. Rasnik, I.; McKinney, S. A.; Ha, T. Nonblinking and long-lasting single-molecule fluorescence
4 imaging. *Nat. Methods* **2006**, *3*, 891-893.
5. Aitken, C. E.; Marshall, R. A.; Puglisi, J. D. An oxygen scavenging system for improvement of dye
6 stability in single-molecule fluorescence experiments. *Biophys. J.* **2008**, *94*, 1826-1835.
7. Benesch, R. E.; Benesch, R. Enzymatic removal of oxygen for polarography and related methods.
8 *Science* **1953**, *118*, 447-448.
9. Swoboda, M.; Henig, J.; Cheng, H.-M.; Brugger, D.; Haltrich, D.; Plumeré, N.; Schlierf, M.
10 Enzymatic Oxygen Scavenging for Photostability without pH Drop in Single-Molecule Experiments. *ACS
11 Nano* **2012**, *6*, 6364-6369.
12. Ha, T.; Tinnefeld, P. Photophysics of fluorescent probes for single-molecule biophysics and super-
13 resolution imaging. *Annu. Rev. Phys. Chem.* **2012**, *63*, 595-617.
14. Vogelsang, J.; Kasper, R.; Steinhauer, C.; Person, B.; Heilemann, M.; Sauer, M.; Tinnefeld, P. A
15 reducing and oxidizing system minimizes photobleaching and blinking of fluorescent dyes. *Angew
16 Chem. Int Ed Engl* **2008**, *47*, 5465-5469.
17. Targowski, P.; Ziętek, B.; Bączyński, A. Luminescence Quenching of Rhodamines by
18 Cyclooctatetraene. In *Zeitschrift für Naturforschung A*, 1987; Vol. 42, p 1009.
19. Heupel, M.; Gregor, I.; Becker, S.; Thiel, E. Photophysical and photochemical properties of
20 electronically excited fluorescent dyes: A new type of time-resolved laser-scanning spectroscopy. *Intl. J.
21 Photoenergy* **1999**, *1*, 165-172.
22. Dave, R.; Terry, D. S.; Munro, J. B.; Blanchard, S. C. Mitigating unwanted photophysical processes
23 for improved single-molecule fluorescence imaging. *Biophys. J.* **2009**, *96*, 2371-2381.
24. Pfiffi, D.; Bier, B. A.; Marian, C. M.; Schaper, K.; Seidel, C. A. M. Diphenylhexatrienes as
25 Photoprotective Agents for Ultrasensitive Fluorescence Detection. *J. Phys. Chem. A* **2010**, *114*, 4099-
26 4108.
27. Glembockyte, V.; Lincoln, R.; Cosa, G. Cy3 photoprotection mediated by Ni²⁺ for extended single-
28 molecule imaging: old tricks for new techniques. *J. Am Chem. Soc.* **2015**, *137*, 1116-1122.
29. Glembockyte, V.; Lin, J.; Cosa, G. Improving the Photostability of Red- and Green-Emissive
30 Single-Molecule Fluorophores via Ni(2+) Mediated Excited Triplet-State Quenching. *J. Phys. Chem. B*
31 **2016**, *120*, 11923-11929.
32. Smit, J. H.; van der Velde, J. H. M.; Huang, J.; Trauschke, V.; Henrikus, S. S.; Chen, S.;
33 Eleftheriadis, N.; Warszawik, E. M.; Herrmann, A.; Cordes, T. On the impact of competing intra- and
34 intermolecular triplet-state quenching on photobleaching and photoswitching kinetics of organic
35 fluorophores. *Phys. Chem. Chem. Phys.* **2019**, *21*, 3721-3733.
36. Cordes, T.; Vogelsang, J.; Tinnefeld, P. On the Mechanism of Trolox as Antiblinking and
37 Antibleaching Reagent. *J. Am Chem. Soc.* **2009**, *131*, 5018-5019.
38. Vogelsang, J.; Cordes, T.; Forthmann, C.; Steinhauer, C.; Tinnefeld, P. Controlling the
39 fluorescence of ordinary oxazine dyes for single-molecule switching and superresolution microscopy.
40 *Proc. Natl. Acad. Sci. USA* **2009**, *106*, 8107-8112.

- 1
2
3 944 17. Cordes, T.; Vogelsang, J.; Steinhauer, C.; Stein, I. H.; Forthmann, C.; Gietl, A.; Schmied, J. J.;
4 945 Acuna, G. P.; Laurien, S.; Lalkens, B.; et al. Far-Field Nanoscopy with Conventional Fluorophores:
5 946 Photostability, Photophysics, and Transient Binding. In *Far-Field Optical Nanoscopy*, Tinnefeld, P.;
6 947 Eggeling, C.; Hell, S. W., Eds. Springer Berlin Heidelberg: Berlin, Heidelberg, 2015; pp 215-242.
7
8 948 18. van der Velde, J. H.; Uusitalo, J. J.; Ugen, L. J.; Warszawik, E. M.; Herrmann, A.; Marrink, S. J.;
9 949 Cordes, T. Intramolecular photostabilization via triplet-state quenching: Design principles to make
10 950 organic fluorophores "self-healing." *Faraday Discuss.* **2015**, *184*, 221-235.
11
12 951 19. van der Velde, J. H.; Oelerich, J.; Huang, J.; Smit, J. H.; Aminian Jazi, A.; Galiani, S.; Kolmakov,
13 952 K.; Guoridis, G.; Eggeling, C.; Herrmann, A.; et al. A simple and versatile design concept for fluorophore
14 953 derivatives with intramolecular photostabilization. *Nat. Commun.* **2016**, *7*, 10144.
15
16 954 20. Alejo, J. L.; Blanchard, S. C.; Andersen, O. S. Small-Molecule Photostabilizing Agents are
17 955 Modifiers of Lipid Bilayer Properties. *Biophys. J.* **2013**, *104*, 2410-2418.
18
19 956 21. Cordes, T.; Santoso, Y.; Tomescu, A. I.; Gryte, K.; Hwang, L. C.; Camara, B.; Wigneshweraraj, S.;
20 957 Kapanidis, A. N. Sensing DNA opening in transcription using quenchable Förster resonance energy
21 958 transfer. *Biochemistry* **2010**, *49*, 9171-9180.
22
23 959 22. Altman, R. B.; Terry, D. S.; Zhou, Z.; Zheng, Q.; Geggier, P.; Kolster, R. A.; Zhao, Y.; Javitch, J. A.;
24 960 Warren, J. D.; Blanchard, S. C. Cyanine fluorophore derivatives with enhanced photostability. *Nat. Methods* **2012**, *9*, 68-71.
25
26 961 23. Zheng, Q.; Jockusch, S.; Zhou, Z.; Altman, R. B.; Warren, J. D.; Turro, N. J.; Blanchard, S. C. On
27 962 the Mechanisms of Cyanine Fluorophore Photostabilization. *J. Phys. Chem. Lett.* **2012**, *3*, 2200-2203.
28
29 963 24. van der Velde, J. H.; Ploetz, E.; Hiermaier, M.; Oelerich, J.; de Vries, J. W.; Roelfes, G.; Cordes, T.
30 964 Mechanism of intramolecular photostabilization in self-healing cyanine fluorophores. *Chemphyschem*
31 965 **2013**, *14*, 4084-4093.
32
33 966 25. Zheng, Q.; Juette, M. F.; Jockusch, S.; Wasserman, M. R.; Zhou, Z.; Altman, R. B.; Blanchard, S.
34 967 C. Ultra-stable organic fluorophores for single-molecule research. *Chem. Soc. Rev.* **2014**, *43*, 1044-
35 968 1056.
36
37 969 26. Liphardt, B.; Liphardt, B.; Lüttke, W. Laser dyes III: Concepts to increase the photostability of laser
38 970 dyes. *Optics Commun.* **1983**, *48*, 129-133.
39
40 971 27. Liphardt, B.; Liphardt, B.; Lüttke, W. Laser dyes with intramolecular triplet quenching. *Optics
41 972 Commun.* **1981**, *38*, 207-210.
42
43 973 28. Altman, R. B.; Zheng, Q.; Zhou, Z.; Terry, D. S.; Warren, J. D.; Blanchard, S. C. Enhanced
44 974 photostability of cyanine fluorophores across the visible spectrum. *Nat. Methods* **2012**, *9*, 428-429.
45
46 975 29. Tinnefeld, P.; Cordes, T. "Self-healing" dyes: Intramolecular stabilization of organic fluorophores.
47
48 976 *Nat. Methods* **2012**, *9*, 426-427; author reply 427-428.
49
50 977 30. Glembockyte, V.; Wieneke, R.; Gatterdam, K.; Gidi, Y.; Tampe, R.; Cosa, G. *Tris-N-Nitritotriacetic
51 978 Acid Fluorophore as a Self-Healing Dye for Single-Molecule Fluorescence Imaging*. *J. Am Chem. Soc*
52 979 **2018**, *140*, 11006-11012.
53
54 980 31. Zheng, Q.; Jockusch, S.; Zhou, Z.; Altman, R. B.; Zhao, H.; Asher, W.; Holsey, M.; Mathiasen, S.;
55 981 Geggier, P.; Javitch, J. A.; et al. Electronic tuning of self-healing fluorophores for live-cell and single-
56 982 molecule imaging. *Chem. Sci.* **2017**, *8*, 755-762.
57
58 983 32. van der Velde, J. H.; Oelerich, J.; Huang, J.; Smit, J. H.; Hiermaier, M.; Ploetz, E.; Herrmann, A.;
59
60

- 1
2
3 985 Roelfes, G.; Cordes, T. The Power of Two: Covalent Coupling of Photostabilizers for Fluorescence
4 986 Applications. *J. Phys. Chem. Lett.* **2014**, *5*, 3792-3798.
5
6 987 33. Zheng, Q.; Jockusch, S.; Rodriguez-Calero, G. G.; Zhou, Z.; Zhao, H.; Altman, R. B.; Abruna, H.
7 988 D.; Blanchard, S. C. Intra-molecular triplet energy transfer is a general approach to improve organic
8 989 fluorophore photostability. *Photochem. Photobiol. Sci.* **2016**, *15*, 196-203.
9
10 990 34. Glembokyte, V.; Cosa, G. Redox-Based Photostabilizing Agents in Fluorescence Imaging: The
11 991 Hidden Role of Intersystem Crossing in Geminate Radical Ion Pairs. *J. Am Chem. Soc* **2017**, *139*,
12 992 13227-13233.
13
14 993 35. van der Velde, J. H. M.; Smit, J. H.; Hebisch, E.; Punter, M.; Cordes, T. Self-healing dyes for
15 994 super-resolution fluorescence microscopy. *J. Phys. D: Applied Phys.* **2019**, *52*, 034001.
16
17 995 36. Schäfer, F. P.; Zhang, F.-G.; Jethwa, J. Intramolecular TT-energy transfer in bifluorophoric laser
18 996 dyes. *Applied Phys. B* **1982**, *28*, 37-41.
19
20 997 37. Li, T.; Liu, L.; Jing, T.; Ruan, Z.; Yuan, P.; Yan, L. Self-Healing Organic Fluorophore of Cyanine-
21 998 Conjugated Amphiphilic Polypeptide for Near-Infrared Photostable Bioimaging. *ACS Applied Mater.*
22 999 *Interfaces* **2018**, *10*, 14517-14530.
23
24 1000 38. Zheng, Q.; Jockusch, S.; Zhou, Z.; Blanchard, S. C. The Contribution of Reactive Oxygen Species
25 1001 to the Photobleaching of Organic Fluorophores. *Photochem. Photobiol.* **2014**, *90*, 448-454.
26
27 1002 39. Stolow, A.; Bragg, A. E.; Neumark, D. M. Femtosecond Time-Resolved Photoelectron
28 1003 Spectroscopy. *Chem. Rev.* **2004**, *104*, 1719-1758.
29
30 1004 40. Burda, C.; El-Sayed, M. A. High-density femtosecond transient absorption spectroscopy of
31 1005 semiconductor nanoparticles. A tool to investigate surface quality. *Pure Applied Chem.* **2000**, *72*, 165-
32 1006 177.
33
34 1007 41. de Boer, M.; Gouridis, G.; Vietrov, R.; Begg, S. L.; Schuurman-Wolters, G. K.; Husada, F.;
35 1008 Eleftheriadis, N.; Poolman, B.; McDevitt, C. A.; Cordes, T. Conformational and dynamic plasticity in
36 1009 substrate-binding proteins underlies selective transport in ABC importers. *eLife* **2019**, *8*, e44652.
37
38 1010 42. Gouridis, G.; Schuurman-Wolters, G. K.; Ploetz, E.; Husada, F.; Vietrov, R.; de Boer, M.; Cordes,
39 1011 T.; Poolman, B. Conformational dynamics in substrate-binding domains influences transport in the ABC
40 1012 importer GlnPQ. *Nat. Struct. Mol. Biol.* **2015**, *22*, 57-64.
41
42 1013 43. Roy, R.; Hohng, S.; Ha, T. A practical guide to single-molecule FRET. *Nat. Methods* **2008**, *5*, 507-
43 1014 516.
44
45 1015 44. Wennmalm, S.; Edman, L.; Rigler, R. Conformational fluctuations in single DNA molecules. *Proc.*
46 1016 *Natl. Acad. Sci. USA* **1997**, *94*, 10641-10646.
47
48 1017 45. Sirbu, D.; Woodford, O. J.; Benniston, A. C.; Harriman, A. Photocatalysis and self-catalyzed
49 1018 photobleaching with covalently-linked chromophore-quencher conjugates built around BOPHY.
50 1019 *Photochem. Photobiol. Sci.* **2018**, *17*, 750-762.
51
52 1020 46. Juette, M. F.; Terry, D. S.; Wasserman, M. R.; Zhou, Z.; Altman, R. B.; Zheng, Q.; Blanchard, S. C.
53 1021 The bright future of single-molecule fluorescence imaging. *Curr. Opin. Chem. Biol.* **2014**, *20*, 103-111.
54
55 1022 47. Weller, A. Photoinduced Electron Transfer in Solution: Exciplex and Radical Ion Pair Formation
56 1023 Free Enthalpies and their Solvent Dependence. In *Zeitschrift für Physikalische Chemie*, 1982; Vol. 133,
57 1024 p 93.
58
59 1025 48. Chandler, D. "Electron transfer in water and other polar environments, how it happens," in
60

- 1
2
3 1026 *Classical and Quantum Dynamics in Condensed Phase Simulations*, eds. Berne, B. J.; Ciccotti, G.;
4 1027 Coker, D. F. (World Scientific: Singapore), 1998, pp 25–49.
5
6 1028 49. Holzmeister, P.; Gietl, A.; Tinnefeld, P. Geminate Recombination as a Photoprotection Mechanism
7 1029 for Fluorescent Dyes. *Angewandte Chem. Intl. Ed.* **2014**, *53*, 5685-5688.
8
9 1030 50. Turro, N. J. *Modern Molecular Photochemistry*. University Science Books: Mill Valley, Calif., 1991.
10
11 1031 51. Frutos, L.-M.; Castaño, O.; Merchán, M. Theoretical Determination of the Singlet → Singlet and
12 1032 Singlet → Triplet Electronic Spectra, Lowest Ionization Potentials, and Electron Affinity of
13 1033 Cyclooctatetraene. *J. Phys. Chem. A* **2003**, *107*, 5472-5478.
14
15 1034 52. Frutos, L. M.; Castaño, O.; Andrés, J. L.; Merchán, M.; Acuna, A. U. A theory of nonvertical triplet
16 1035 energy transfer in terms of accurate potential energy surfaces: The transfer reaction from π,π^* triplet
17 1036 donors to 1,3,5,7-cyclooctatetraene. *J. Chem. Phys.* **2004**, *120*, 1208-1216.
18
19 1037 53. Wagner, P. J.; Klán, P. Intramolecular Triplet Energy Transfer in Flexible Molecules: Electronic,
20 1038 Dynamic, and Structural Aspects. *J. Am. Chem. Soc.* **1999**, *121*, 9626-9635.
21
22 1039 54. Hell, S. W.; Sahl, S. J.; Bates, M.; Zhuang, X.; Heintzmann, R.; Booth, M. J.; Bewersdorf, J.;
23 1040 Shtengel, G.; Hess, H.; Tinnefeld, P.; et al. The 2015 super-resolution microscopy roadmap. *J. Phys. D: Applied Phys.* **2015**, *48*, 443001.
24
25
26 1042 55. Heilemann, M.; Margeat, E.; Kasper, R.; Sauer, M.; Tinnefeld, P. Carbocyanine Dyes as Efficient
27 1043 Reversible Single-Molecule Optical Switch. *J. Am. Chem. Soc.* **2005**, *127*, 3801-3806.
28
29 1044 56. Bates, M.; Blosser, T. R.; Zhuang, X. Short-range spectroscopic ruler based on a single-molecule
30 1045 optical switch. *Phys. Rev. Lett.* **2005**, *94*, 108101.
31
32 1046 57. van de Linde, S.; Löschberger, A.; Klein, T.; Heidbreder, M.; Wolter, S.; Heilemann, M.; Sauer, M.
33 1047 Direct stochastic optical reconstruction microscopy with standard fluorescent probes. *Nat. Protocols*
34 1048 **2011**, *6*, 991-1009.
35
36 1049 58. Vaughan, J. C.; Dempsey, G. T.; Sun, E.; Zhuang, X. Phosphine Quenching of Cyanine Dyes as a
37 1050 Versatile Tool for Fluorescence Microscopy. *J. Am. Chem. Soc.* **2013**, *135*, 1197-1200.
38
39 1051 59. Heilemann, M.; van de Linde, S.; Mukherjee, A.; Sauer, M. Super-Resolution Imaging with Small
40 1052 Organic Fluorophores. *Angewandte Chem. Intl. Ed.* **2009**, *48*, 6903-6908.
41
42 1053 60. Rust, M. J.; Bates, M.; Zhuang, X. Sub-diffraction-limit imaging by stochastic optical reconstruction
43 1054 microscopy (STORM). *Nat. Methods* **2006**, *3*, 793-795.
44
45 1055 61. Bates, M.; Blosser, T. R.; Zhuang, X. Short-range spectroscopic ruler based on a single-molecule
46 1056 optical switch. *Phys. Rev. Lett.* **2005**, *94*, 108101.
47
48 1057 62. Dempsey, G. T.; Vaughan, J. C.; Chen, K. H.; Bates, M.; Zhuang, X. Evaluation of fluorophores for
49 1058 optimal performance in localization-based super-resolution imaging. *Nat. Methods* **2011**, *8*, 1027-1036.
50
51 1059 63. Lakowicz, J. R.; Weber, G. Quenching of fluorescence by oxygen. Probe for structural fluctuations
52 1060 in macromolecules. *Biochemistry* **1973**, *12*, 4161-4170.
53
54 1061 64. Monti, S.; Gardini, E.; Bortolus, P.; Amouyal, E. The triplet state of azobenzene. *Chem. Phys. Lett.*
55 1062 **1981**, *77*, 115-119.
56
57 1063 65. Levitus, M.; Ranjit, S. Cyanine dyes in biophysical research: the photophysics of polymethine
58 1064 fluorescent dyes in biomolecular environments. *Quart. Rev. Biophys.* **2011**, *44*, 123-151.
59
60 1065 66. Sanborn, M. E.; Connolly, B. K.; Gurunathan, K.; Levitus, M. Fluorescence Properties and
Photophysics of the Sulfoindocyanine Cy3 Linked Covalently to DNA. *J. Phys. Chem. B* **2007**, *111*,

- 1
2
3 1067 11064-11074.
4
5 1068 67. Doose, S.; Neuweiler, H.; Sauer, M. Fluorescence quenching by photoinduced electron transfer: a
6 reporter for conformational dynamics of macromolecules. *Chemphyschem* **2009**, *10*, 1389-1398.
7
8 1070 68. Seidel, C. A. M.; Schulz, A.; Sauer, M. H. M. Nucleobase-Specific Quenching of Fluorescent Dyes.
9
10 1071 1. Nucleobase One-Electron Redox Potentials and Their Correlation with Static and Dynamic Quenching
11 Efficiencies. *J. Phys. Chem.* **1996**, *100*, 5541-5553.
12
13 1073 69. Heinlein, T.; Knemeyer, J.-P.; Piestert, O.; Sauer, M. Photoinduced electron transfer between
14 fluorescent dyes and guanosine residues in DNA-hairpins. *J. Phys. Chem. B* **2003**, *107*, 7957-7964.
15
16 1075 70. Vogelsang, J.; Cordes, T.; Tinnefeld, P. Single-molecule photophysics of oxazines on DNA and its
17 application in a FRET switch. *Photochem. Photobiol. Sci.* **2009**, *8*, 486-496.
18
19 1077 71. Spiriti, J.; Binder, J. K.; Levitus, M.; van der Vaart, A. Cy3-DNA stacking interactions strongly
20 depend on the identity of the terminal basepair. *Biophys. J.* **2011**, *100*, 1049-1057.
21
22 1079 72. Ranjit, S.; Levitus, M. Probing the interaction between fluorophores and DNA nucleotides by
23 fluorescence correlation spectroscopy and fluorescence quenching. *Photochem. Photobiol.* **2012**, *88*,
24 1081 782-791.
25
26 1082 73. Sánchez-Rico, C.; Voith von Voithenberg, L.; Warner, L.; Lamb, D. C.; Sattler, M. Effects of
27 Fluorophore Attachment on Protein Conformation and Dynamics Studied by spFRET and NMR
28 Spectroscopy. *Chem. Eur. J.* **2017**, *23*, 14267-14277.
29
30 1085 74. Tsunoyama, T. A.; Watanabe, Y.; Goto, J.; Naito, K.; Kasai, R. S.; Suzuki, K. G. N.; Fujiwara, T. K.;
31 Kusumi, A. Super-long single-molecule tracking reveals dynamic-anchorage-induced integrin function.
32
33 1088 75. Reilly, D. T.; Kim, S. H.; Katzenellenbogen, J. A.; Schroeder, C. M. Fluorescent Nanoconjugate
34 Derivatives with Enhanced Photostability for Single Molecule Imaging. *Anal. Chem.* **2015**, *87*, 11048-
35 1090 11057.
36
37 1091 76. García-López, V.; Jeffet, J.; Kuwahara, S.; Martí, A.; Ebenstein, Y.; Tour, J. Synthesis and
38 Photostability of Unimolecular Submersible Nanomachines: Toward Single-Molecule Tracking in
39 Solution. *Org. Lett.* **2016**, *18*, 2343-2346.
40
41 1094 77. Cordes, T.; Maiser, A.; Steinhauer, C.; Schermelleh, L.; Tinnefeld, P. Mechanisms and
42 advancement of antifading agents for fluorescence microscopy and single-molecule spectroscopy. *Phys.*
43
44 1096 *Chem. Phys. Chem.* **2011**, *13*, 6699-6709.
45
46 1097 78. Danzl, J. G.; Sidenstein, S. C.; Gregor, C.; Urban, N. T.; Ilgen, P.; Jakobs, S.; Hell, S. W.
47 Coordinate-targeted fluorescence nanoscopy with multiple off states. *Nat. Photon.* **2016**, *10*, 122-128.
48
49 1099 79. Balzarotti, F.; Eilers, Y.; Gwosch, K. C.; Gynnå, A. H.; Westphal, V.; Stefani, F. D.; Elf, J.; Hell, S.
50 W. Nanometer resolution imaging and tracking of fluorescent molecules with minimal photon fluxes.
51
52 1102 80. Lerner, E.; Cordes, T.; Ingargiola, A.; Alhadid, Y.; Chung, S.; Michalet, X.; Weiss, S. Toward
53 dynamic structural biology: Two decades of single-molecule Förster resonance energy transfer. *Science*
54 **2018**, *359*, eaan1133.
55
56 1105 81. Hohlbein, J.; Craggs, T. D.; Cordes, T. Alternating-laser excitation: single-molecule FRET and
57 beyond. *Chem. Soc. Rev.* **2014**, *43*, 1156-1171.
58
59 1107 82. Kapanidis, A.; Majumdar, D.; Heilemann, M.; Nir, E.; Weiss, S. Alternating Laser Excitation for
60

- 1
2
3 1108 Solution-Based Single-Molecule FRET. *Cold Spring Harb. Protocols.* **2015**, , 979-87.
4
5 1109 83. Munro, J. B.; Altman, R. B.; Tung, C.-S.; Cate, J. H. D.; Sanbonmatsu, K. Y.; Blanchard, S. C.
6 1110 Spontaneous formation of the unlocked state of the ribosome is a multistep process. *Proc. Natl. Acad.*
7 1111 *Sci. USA* **2010**, *107* (2), 709-714.
8
9 1112 84. Shank, N. I.; Zanotti, K. J.; Lanni, F.; Berget, P. B.; Armitage, B. A. Enhanced Photostability of
10 1113 Genetically Encodable Fluoromodules Based on Fluorogenic Cyanine Dyes and a Promiscuous Protein
11 1114 Partner. *J. Am. Chem. Soc.* **2009**, *131*, 12960-12969.
12
13 1115 85. Shank, N. I.; Pham, H. H.; Waggoner, A. S.; Armitage, B. A. Twisted Cyanines: A Non-Planar
14 1116 Fluorogenic Dye with Superior Photostability and Its Use in a Protein-Based Fluoromodule. *J. Am.*
15 1117 *Chem. Soc.* **2013**, *135*, 242-251.
16
17 1118 86. Renikuntla, B. R.; Rose, H. C.; Eldo, J.; Waggoner, A. S.; Armitage, B. A. Improved Photostability
18 1119 and Fluorescence Properties through Polyfluorination of a Cyanine Dye. *Org. Lett.* **2004**, *6*, 909-912.
19
20 1120 87. Funabiki, K.; Yagi, K.; Ueta, M.; Nakajima, M.; Horiuchi, M.; Kubota, Y.; Mastui, M. Rational
21 1121 Molecular Design and Synthesis of Highly Thermo- and Photostable Near-Infrared-Absorbing
22 1122 Heptamethine Cyanine Dyes with the Use of Fluorine Atoms. *Chemistry* **2016**, *22*, 12282-12285.
23
24 1123 88. Yang, S. K.; Shi, X.; Park, S.; Ha, T.; Zimmerman, S. C. A dendritic single-molecule fluorescent
25 1124 probe that is monovalent, photostable and minimally blinking. *Nat. Chem.* **2013**, *5*, 692-697.
26
27 1125 89. Yang, S. K.; Shi, X.; Park, S.; Doganay, S.; Ha, T.; Zimmerman, S. C. Monovalent, Clickable,
28 1126 Uncharged, Water-Soluble Perylenediimide-Cored Dendrimers for Target-Specific Fluorescent
29 1127 Biolabeling. *J. Am. Chem. Soc.* **2011**, *133*, 9964-9967.
30
31 1128 90. Redy-Keisar, O.; Huth, K.; Vogel, U.; Lepenies, B.; Seeberger, P. H.; Haag, R.; Shabat, D.
32 1129 Enhancement of fluorescent properties of near-infrared dyes using clickable oligoglycerol dendrons.
33 1130 *Org. Biomol. Chem.* **2015**, *13*, 4727-4732.
34
35 1131 91. Mohanty, J.; Nau, W. M. Ultrastable Rhodamine with Cucurbituril. *Angewandte Chem. Intl. Ed.*
36 1132 **2005**, *44*, 3750-3754.
37
38 1133 92. Guether, R.; Reddington, M. V. Photostable Cyanine Dye β -Cyclodextrin Conjugates. *Tetrahedron*
39 1134 *Lett.* **1997**, *38*, 6167-6170.
40
41 1135 93. Yau, C. M.; Pascu, S. I.; Odom, S. A.; Warren, J. E.; Klotz, E. J.; Frampton, M. J.; Williams, C. C.;
42 1136 Coropceanu, V.; Kuimova, M. K.; Phillips, D.; et al. Stabilisation of a heptamethine cyanine dye by
43 1137 rotaxane encapsulation. *Chem. Commun.* **2008**, 2897-2899.
44
45 1138 94. Sokolov, K.; Chumanov, G.; Cotton, T. M. Enhancement of Molecular Fluorescence Near the
46 1139 Surface of Colloidal Metal Films. *Anal. Chem.* **1998**, *70*, 3898-3905.
47
48 1140 95. Kawakami, T.; Takahashi, Y.; Tatsuma, T. Enhancement of Dye-Sensitized Photocurrents by Gold
49 1141 Nanoparticles: Effects of Plasmon Coupling. *J. Phys. Chem. C* **2013**, *117*, 5901-5907.
50
51 1142 96. Zijlstra, P.; Orrit, M. Single metal nanoparticles: optical detection, spectroscopy and applications.
52 1143 *Rep. Prog. Phys.* **2011**, *74*, 106401.
53
54 1144 97. Acuna, G. P.; Moller, F. M.; Holzmeister, P.; Beater, S.; Lalkens, B.; Tinnefeld, P. Fluorescence
55 1145 enhancement at docking sites of DNA-directed self-assembled nanoantennas. *Science* **2012**, *338*, 506-
56 1146 510.
57
58 1147 98. Grabenhorst, L.; Trofymchuk, K.; Steiner, F.; Glembockyte, V.; Tinnefeld, P. Fluorophore
59 1148 photostability and saturation in the hotspot of DNA origami nanoantennas. *Methods Appl. Fluor.* **2020**, *8*,

- 1
2
3 1149 024003.
4
5 1150 99. Grimm, J. B.; Muthusamy, A. K.; Liang, Y.; Brown, T. A.; Lemon, W. C.; Patel, R.; Lu, R.; Macklin,
6 J. J.; Keller, P. J.; Ji, N.; et al. A general method to fine-tune fluorophores for live-cell and in vivo
7 imaging. *Nat. Methods* **2017**, *14*, 987-994.
8
9 1153 100. Sun, W.-C.; Gee, K. R.; Haugland, R. P. Synthesis of novel fluorinated coumarins: Excellent UV-
10 light excitable fluorescent dyes. *Bioorg. Med. Chem. Lett.* **1998**, *8*, 3107-3110.
11
12 1155 101. Samanta, A.; Vendrell, M.; Das, R.; Chang, Y.-T. Development of photostable near-infrared
13 cyanine dyes. *Chem. Commun.* **2010**, *46*, 7406-7408.
14
15 1157 102. Su, D.; Teoh, C. L.; Samanta, A.; Kang, N.-Y.; Park, S.-J.; Chang, Y.-T. The development of a
16 highly photostable and chemically stable zwitterionic near-infrared dye for imaging applications. *Chem.*
17 *Commun.* **2015**, *51*, 3989-3992.
18
19 1160 103. Butkevich, A. N.; Bossi, M. L.; Lukinavičius, G. v.; Hell, S. W. Triarylmethane Fluorophores
20 Resistant to Oxidative Photobluing. *J. Am. Chem. Soc.* **2018**, *141*, 981-989.
21
22 1162 104. Hendrikus, S.; Tassis, K.; Zhang, L.; van der Velde, J.; Gebhardt, C.; Herrmann, A.; Jung, G.;
23 Cordes, T. Characterization of fluorescent proteins with intramolecular photostabilization. *bioRxiv* **2020**,
24 doi:10.1101/2020.03.07.980722
25
26 1165 105. Byrdin, M.; Duan, C.; Bourgouis, D.; Brettel, K. A Long-Lived Triplet State Is the Entrance Gateway
27 to Oxidative Photochemistry in Green Fluorescent Proteins. *J. Am. Chem. Soc.* **2018**, *140*, 2897-2905.
28
29 1167
30
31
32
33
34
35
36
37
38
39
40
41
42
43
44
45
46
47
48
49
50
51
52
53
54
55
56
57
58
59
60

1168 Short CVs**1169 Michael Isselstein**

1170 Michael Isselstein studied Physics (B.Sc. and M.Sc.) at the Ludwig-Maximilians-Universität (LMU)
1171 in Munich, Germany with a focus on biophysics and microscopy. He is currently working as a PhD
1172 student in the lab of Thorben Cordes at the LMU Munich since 2017. His research is focused on
1173 developing novel fluorescent probes and methods for single molecule studies of membrane
1174 transporter function.



1175

1176

1177 Lei Zhang

1178 Lei Zhang is a Humboldt postdoctoral Research Fellow in Prof. Dr. Thorben Cordes' group at
1179 Ludwig-Maximilians-Universität München (Germany). She studied chemistry in Nanjing Normal
1180 University (China) and obtained a M.S. degree in Chemistry from Xiamen University (China) in
1181 2012 and a PhD degree in Chemistry from Nanjing University (China) in 2015. Her current
1182 research interest are the development of novel fluorescent probes and biophysical assays.



1183

1184

1185 Viktorija Glembockyte

1186 Viktorija Glembockyte is currently a Humboldt Research Fellow at Ludwig-Maximilians-
1187 Universität München (Germany). She studied Chemistry at Jacobs University Bremen (Germany)
1188 and obtained a PhD in Chemistry from McGill University (Canada) in 2017. During her PhD studies
1189 she investigated photophysical properties of fluorophores used for single-molecule fluorescence
1190 imaging applications and developed strategies to improve the photostability of fluorophores. In
1191 her current research she combines the advantages of DNA nanotechnology and single-molecule
1192 fluorescence imaging for the development of diagnostic tools and tunable biosensors.



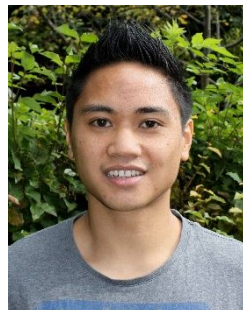
1193

1
2
3
4
5
6
7
8
9
10
11
12
13
14
15
16
17
18
19
20
21
22
23
24
25
26
27
28
29
30
31
32
33
34
35
36
37
38
39
40
41
42
43
44
45
46
47
48
49
50
51
52
53
54
55
56
57
58
59
60

1194

Oliver Brix

1195 Oliver Brix is a PhD student within the research group “Physical and Synthetic Biology” at Ludwig-Maximilians-Universität München (LMU Munich, Germany). He studied Physics at the LMU Munich and the University of Cambridge in the UK. Currently, his main research interests are the advancement of fluorophore photostability and characterizing photodamage in DNA.



1200

1201

Gonzalo Cosa

1202 Gonzalo Cosa received his Licenciate in Chemistry from Universidad Nacional de Rio Cuarto, Argentina, in 1996. He went on to pursue a Ph.D. at the University of Ottawa. He was a postdoctoral fellow at the University of Texas at Austin. In 2005, he joined the Department of Chemistry at McGill University. His current research centers in designing, preparing and utilizing smart fluorescent probes for live cell-imaging and on applying state-of-the-art single-molecule fluorescence methodologies to study protein/DNA/lipid interactions.



1209

1210

Philip Tinnefeld

1211 Philip Tinnefeld is Professor of Physical Chemistry at Ludwig-Maximilians-University since 2017. He studied chemistry in Münster and Heidelberg and received his PhD from the University of Heidelberg in 2002. After postdoctoral work with research stays at UCLA (USA) and Leuven (Belgium) and habilitation in physics at Bielefeld University he became associate professor of biophysics at Ludwig-Maximilians-Universität Munich. In 2010, he was appointed full professor of biophysical chemistry at Braunschweig University of Technology. Philip Tinnefeld's research is inspired by our emerging abilities to study and built matter bottom-up, starting from single molecules. He has contributed to breakthroughs of single-molecule superresolution microscopy and he combined optical single-molecule detection with DNA nanotechnology for self-assembled, functional devices including energy transfer switches, calibration nanorulers, nano-adapters, fluorescence signal amplifiers and molecular force clamps. Dr. Tinnefeld has authored more than 160 publications and patents. He was initiator of GATTQuant GmbH, the first company commercializing DNA origami applications.



1225

1226

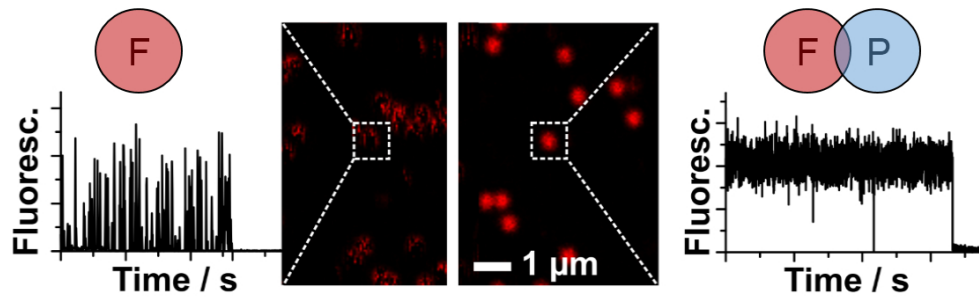
1227 **Thorben Cordes**

1228 Thorben Cordes is currently a Professor for "Physical and Synthetic Biology" at Ludwig-
1229 Maximilians-Universität München (Germany). He studied chemistry at TU Braunschweig
1230 (Germany) and obtained a PhD in Physics from the Ludwig-Maximilians-Universität München
1231 (Germany) in 2008. As a postdoctoral researcher he worked in Munich (Germany) and Oxford
1232 (UK), where he applied single-molecule and super-resolution fluorescence microscopy
1233 techniques to various biological questions. From 2011-2017 has was a tenure-track Assistant
1234 Professor and later tenured Associate Professor at the Zernike Institute for Advanced Materials
1235 at the University of Groningen (The Netherlands). His research interests are structure-function
1236 relationships and molecular mechanisms of membrane transporters and the development of
1237 novel photophysical assays as well as fluorescent probes.

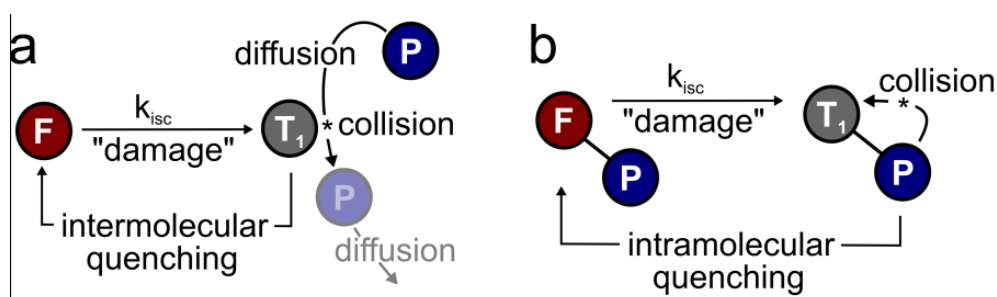


1238

1239

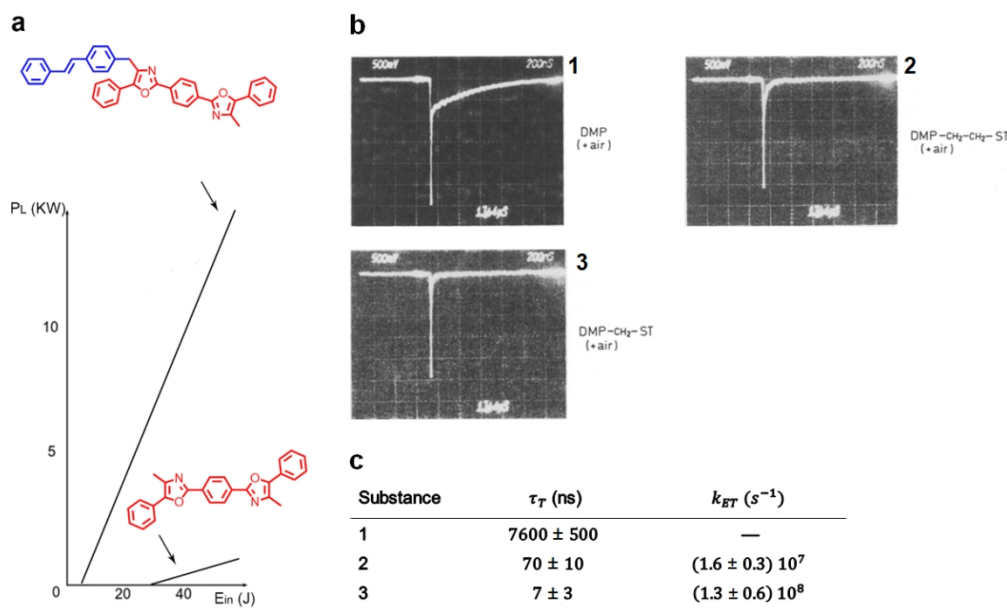


toc figure



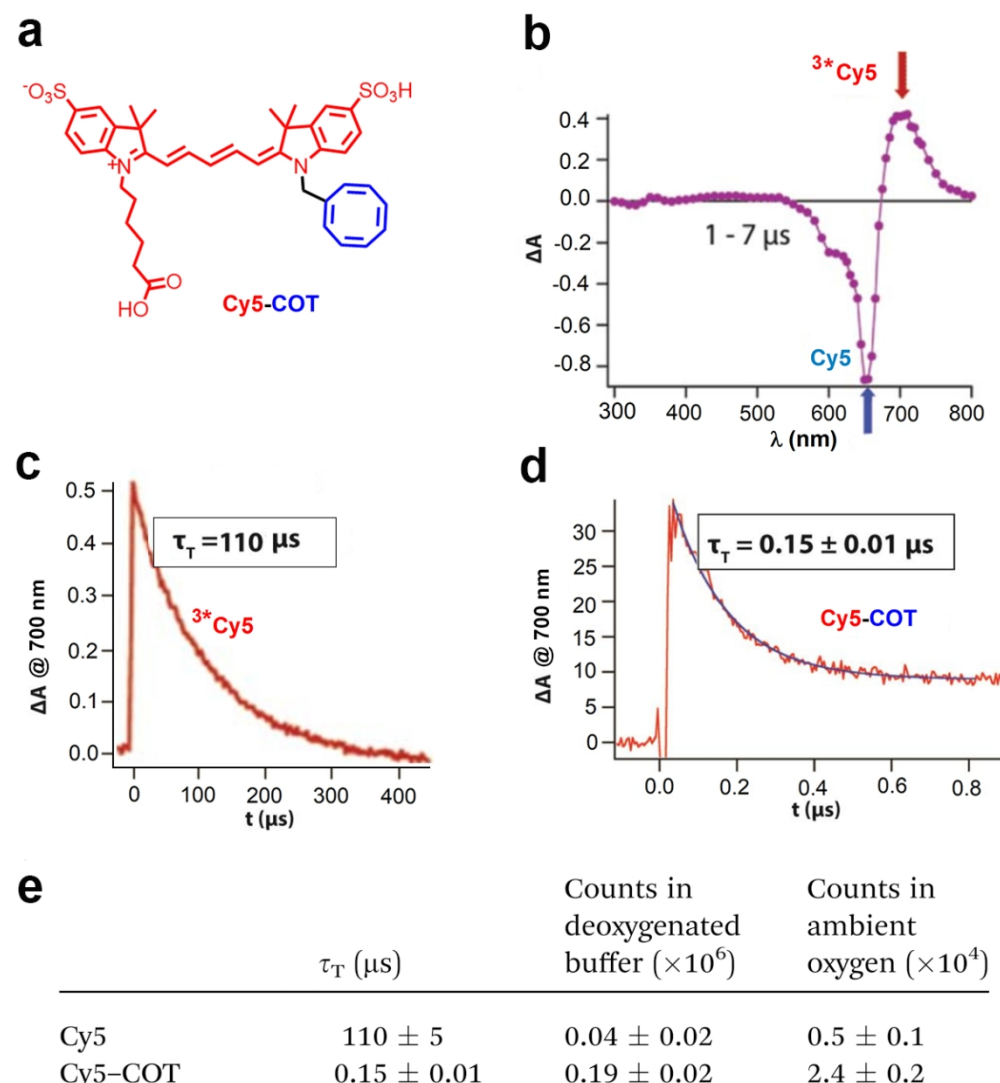
figure

105x31mm (220 x 220 DPI)

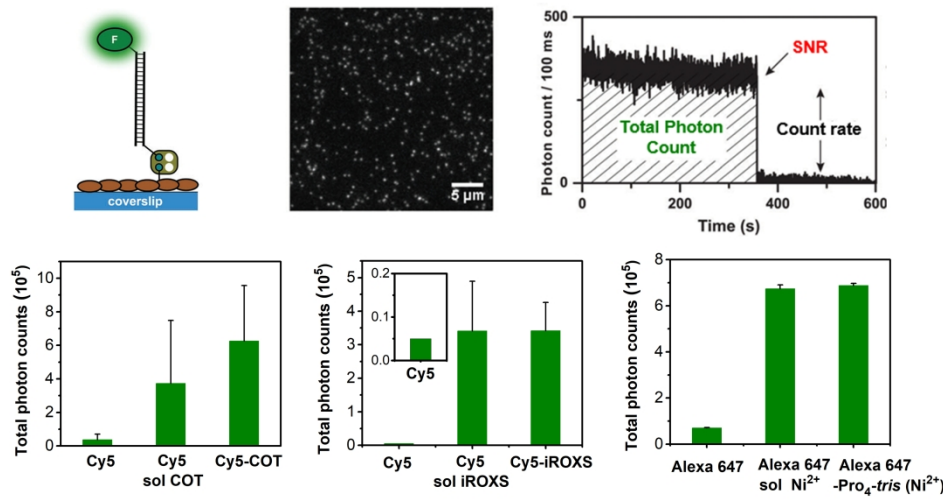


figure

101x61mm (300 x 300 DPI)

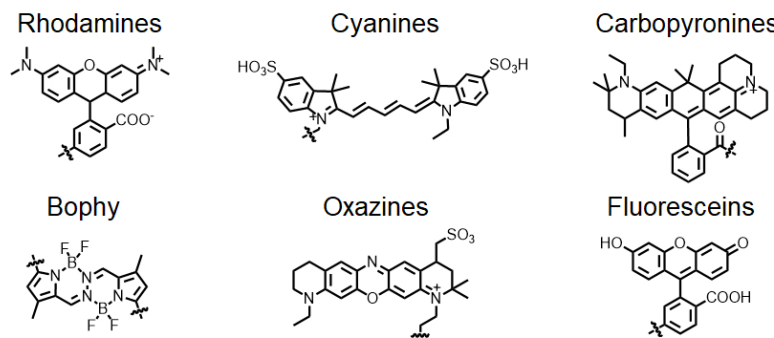
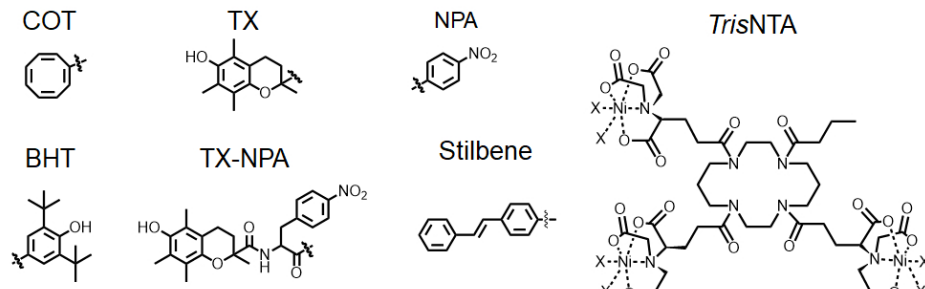


figure



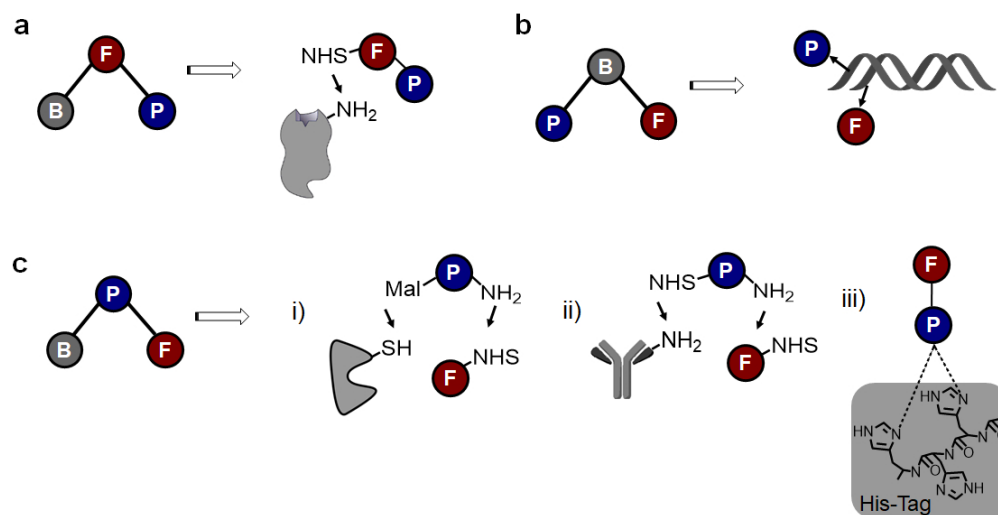
figure

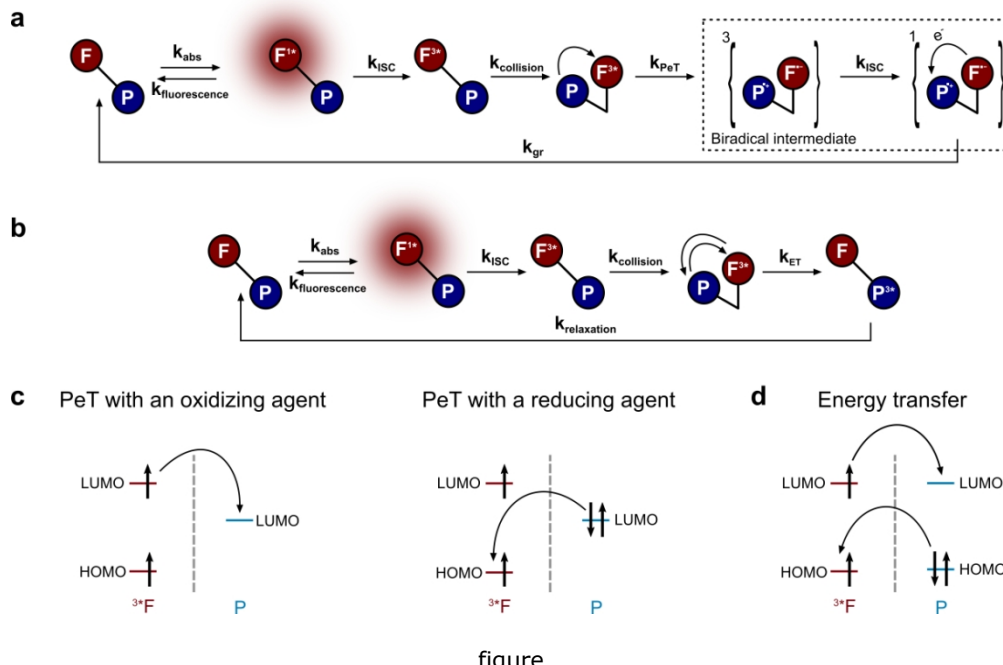
338x190mm (300 x 300 DPI)

a Fluorescent dyes**b Photostabilizers**

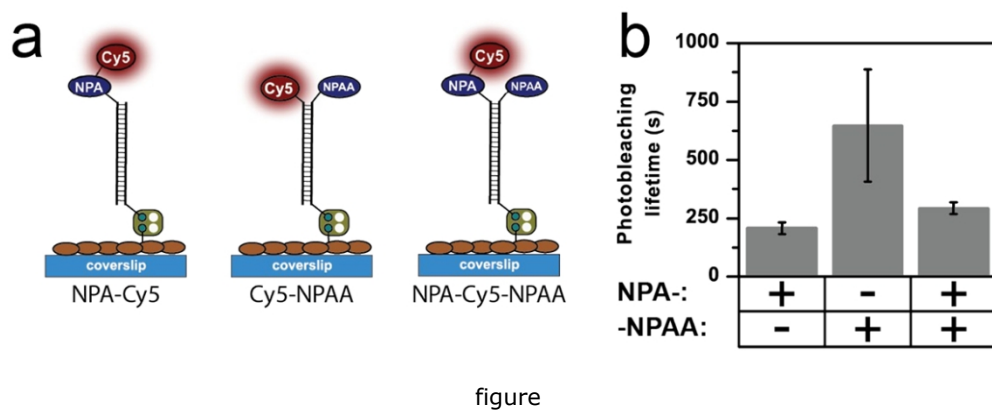
figure

88x73mm (300 x 300 DPI)



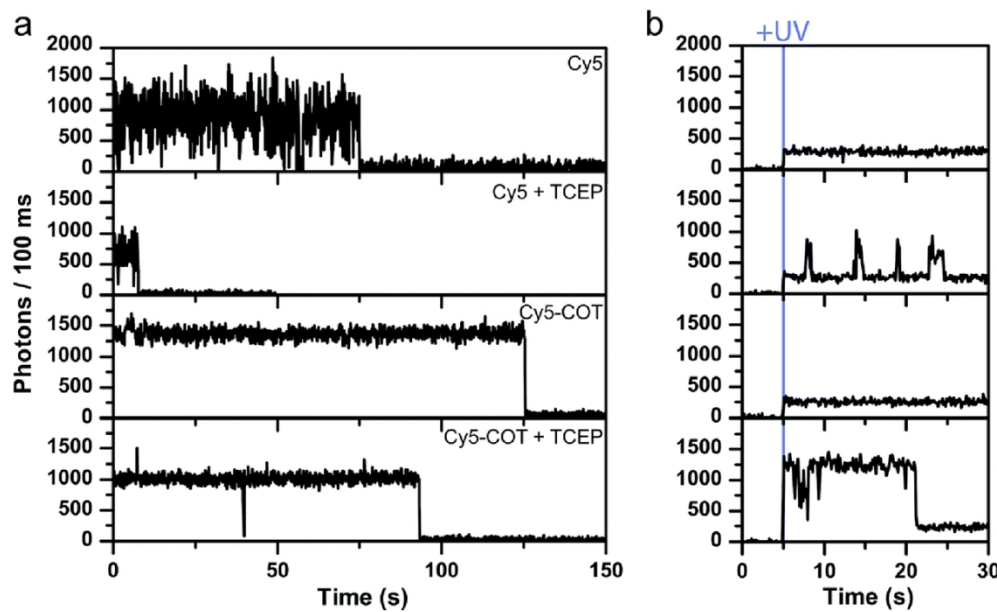


105x66mm (300 x 300 DPI)



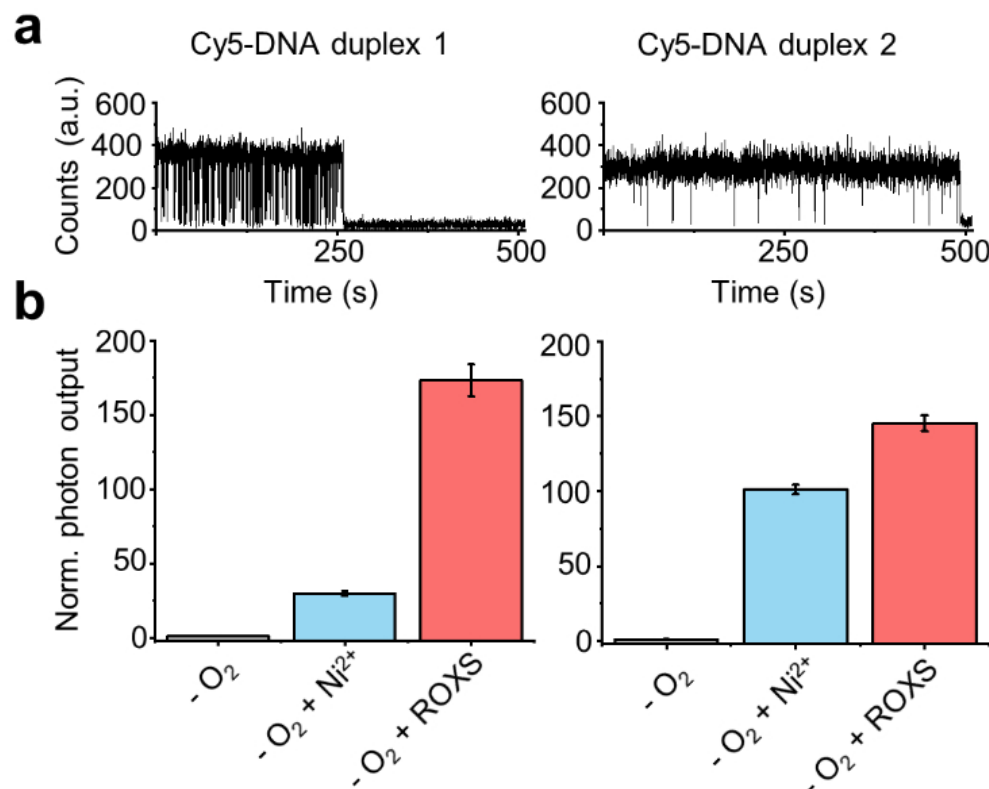
figure

99x34mm (300 x 300 DPI)



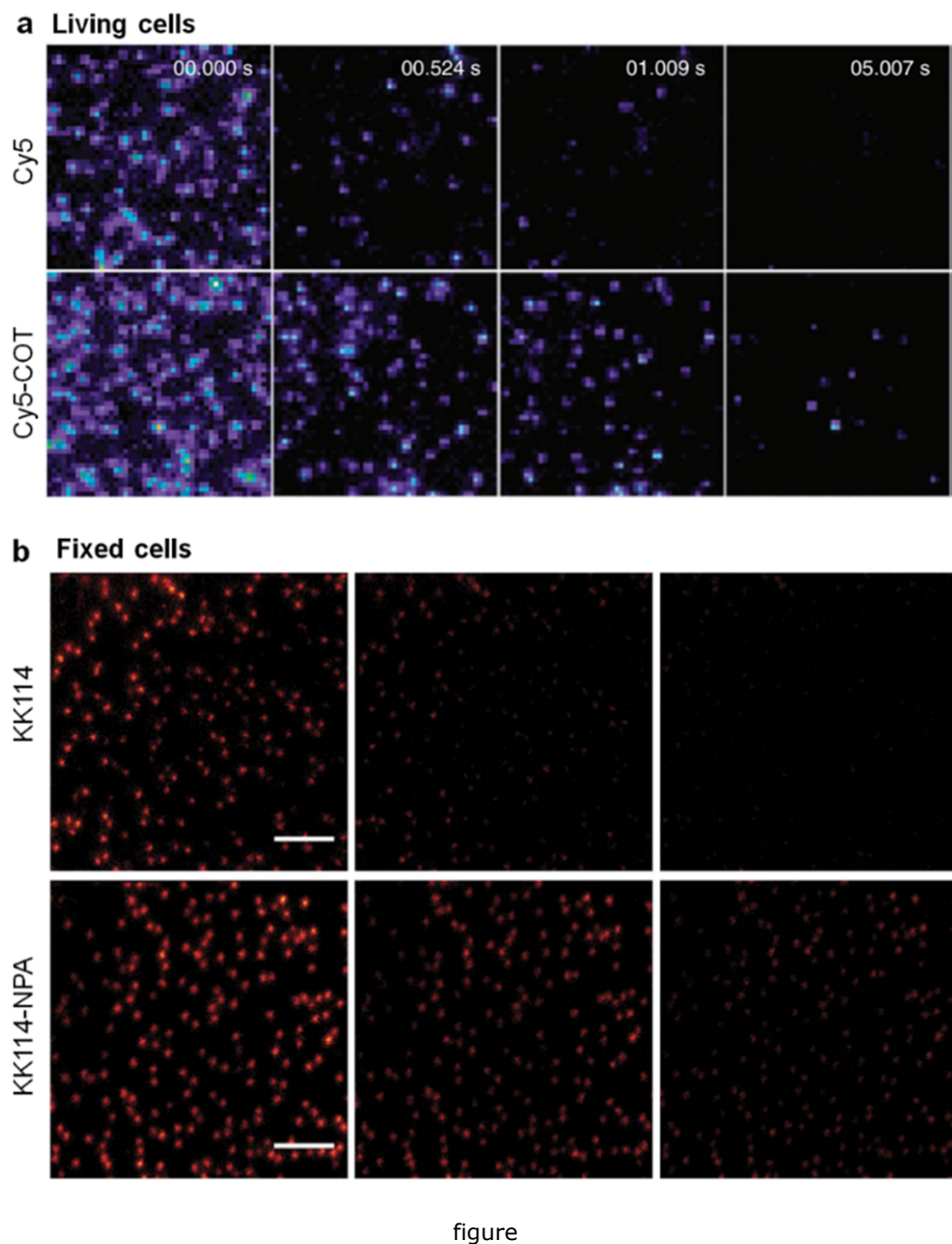
figure

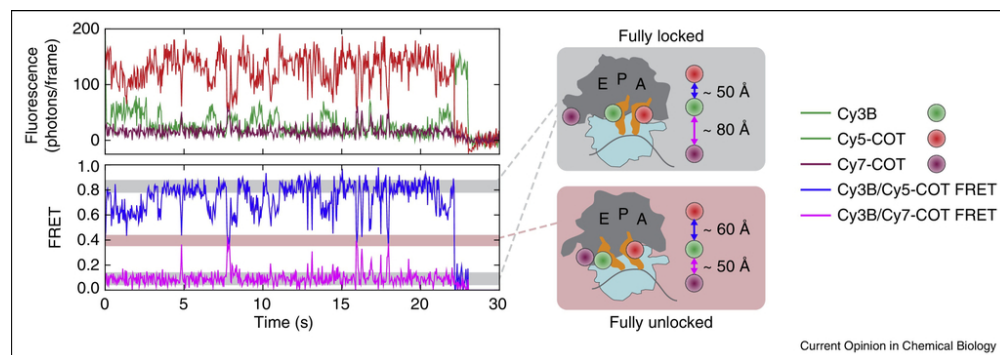
109x66mm (300 x 300 DPI)



figure

85x94mm (220 x 220 DPI)

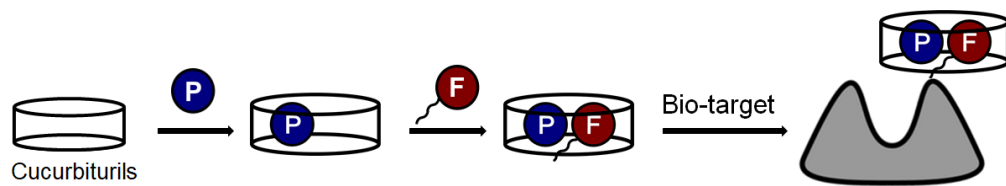




figure

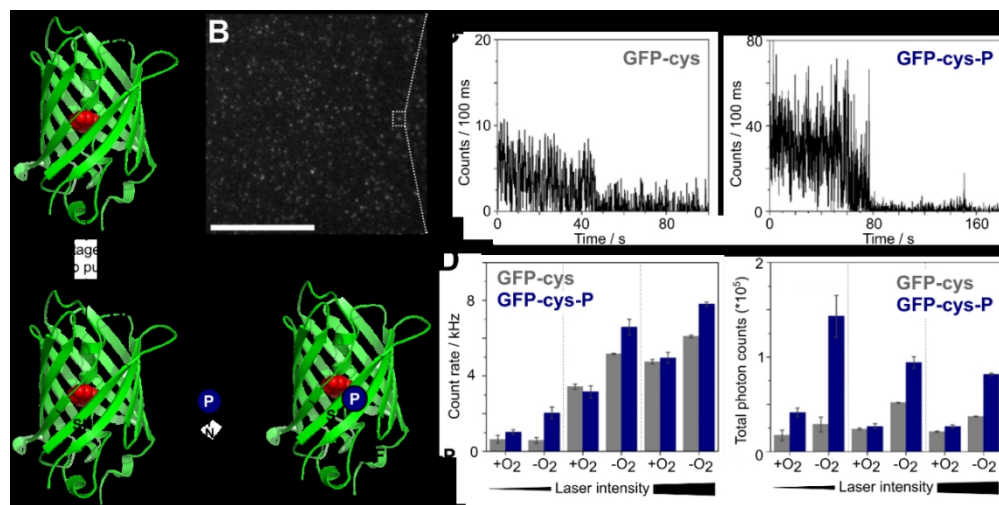
86x30mm (300 x 300 DPI)

Current Opinion in Chemical Biology



figure

100x19mm (300 x 300 DPI)



figure

148x74mm (220 x 220 DPI)